(2)

NRL Memorandum Report 5347

Vibrational Energy Relaxation and Dissociation in N_2

A. W. ALI

Plasma Physics Division

S. SLINKER

JAYCOR, Inc.
Alexandria, VA 22304

June 28, 1984

This report was supported by the Defense Advanced Research Projects Agency (DoD), ARPA Order No. 4395, Amendment No. 33, monitored by the Naval Surface Weapons Center under Contract No. N60921-84-WR-W0131.

NAVAL RESEARCH LABORATORY
Washington, D.C.

SECURITY CLASSIFICATION OF THIS PAGE

REPORT DOCUMENTATION PAGE

1a. REPORT SECURITY CLASSIFICATION **UNCLASSIFIED**	1b. RESTRICTIVE MARKINGS
2a. SECURITY CLASSIFICATION AUTHORITY	3. DISTRIBUTION/AVAILABILITY OF REPORT **Approved for public release; distribution unlimited.**
2b. DECLASSIFICATION/DOWNGRADING SCHEDULE	
4. PERFORMING ORGANIZATION REPORT NUMBER(S) **NRL Memorandum Report 5347**	5. MONITORING ORGANIZATION REPORT NUMBER(S)
6a. NAME OF PERFORMING ORGANIZATION **Naval Research Laboratory** 6b. OFFICE SYMBOL (If applicable) **Code 4700.1**	7a. NAME OF MONITORING ORGANIZATION **Naval Surface Weapons Center**
6c. ADDRESS (City, State and ZIP Code) **Washington, DC 20375**	7b. ADDRESS (City, State and ZIP Code) **Silver Spring, MD 20910**
8a. NAME OF FUNDING/SPONSORING ORGANIZATION **DARPA** 8b. OFFICE SYMBOL (If applicable)	9. PROCUREMENT INSTRUMENT IDENTIFICATION NUMBER
8c. ADDRESS (City, State and ZIP Code) **Arlington, VA 22209**	10. SOURCE OF FUNDING NOS. PROGRAM ELEMENT NO. **60921** / PROJECT NO. / TASK NO. / WORK UNIT NO. **DN680-415**
11. TITLE (Include Security Classification) **Vibrational Energy Relaxation and Dissociation in N_2**	
12. PERSONAL AUTHOR(S) **Ali, A.W. and Slinker, S.***	
13a. TYPE OF REPORT **Interim** 13b. TIME COVERED FROM **1983** TO **1984**	14. DATE OF REPORT (Yr., Mo., Day) **June 28, 1984** 15. PAGE COUNT **55**
16. SUPPLEMENTARY NOTATION ***JAYCOR, Inc., Alexandria, VA 22304** **(Continues)**	
17. COSATI CODES FIELD / GROUP / SUB. GR.	18. SUBJECT TERMS (Continue on reverse if necessary and identify by block number) **Vibrational Relaxation, Nitrogen molecule, Dissociation, Electron-molecule collisions** **(Continues)**

19. ABSTRACT (Continue on reverse if necessary and identify by block number)

A master equation is solved for a nitrogen discharge to determine the vibrational energy relaxation and dissociation. The master equation includes the effects of electron collisions with the molecule, the vibrational-vibrational energy exchange and vibrational-translational energy conversion between the molecules. The establishment of a vibrational distribution is described by a vibrational temperature which is nearly Boltzman and its obtained from the density of 31 vibrational levels. For most conditions the dissociation rate via the vibrational ladder is higher for higher vibrational temperatures. The vibrational temperature is generally depressed due to V-V and T-V effects.

20. DISTRIBUTION/AVAILABILITY OF ABSTRACT UNCLASSIFIED/UNLIMITED X SAME AS RPT ☐ DTIC USERS ☐	21. ABSTRACT SECURITY CLASSIFICATION **UNCLASSIFIED**
22a. NAME OF RESPONSIBLE INDIVIDUAL **A. W. Ali**	22b. TELEPHONE NUMBER (Include Area Code) **(202) 767-3762** 22c. OFFICE SYMBOL **Code 4700.1**

DD FORM 1473, 83 APR EDITION OF 1 JAN 73 IS OBSOLETE

SECURITY CLASSIFICATION OF THIS PAGE

16. SUPPLEMENTARY NOTATION (Continued)

This report was supported by the Defense Advanced Research Projects Agency (DoD), ARPA Order No. 4395, Amendment No. 33, monitored by the Naval Surface Weapons Center under Contract No. N60921-84-WR-W0131.

18. SUBJECT TERMS (Continued)

Vibrational-Vibrational energy exchange

CONTENTS

VIBRATIONAL ENERGY RELAXATION AND DISSOCIATION IN N_2

1. INTRODUCTION

In a nitrogen plasma (N_2) a fair portion of the electron energy is stored in the vibrational mode of the molecules. This energy storage occurs as a result of the electron impact excitations of the various vibrational levels of the molecule, i.e. e-V transitions, as well as by the collisions between the molecules themselves. These collisions result in the energy exchange between the vibrational and translational modes of the molecules, i.e. V-T transitions. The vibrational energy distribution, however, is also affected by the vibrational energy exchange between the molecules through the V-V transitions.

The vibrational energy in a nitrogen plasma has two interesting channels through which the energy is expended, albiet at different time scales. These channels are: the dissociation of the molecule through the vibrational ladder and the other is the vibrational relaxation to the gas kinetic mode. Nitrogen plasmas can be generated by various means, such as microwave and electric discharges, shock waves and by intense electron beams. However, several intrinsic questions arise in such plasmas, namely, what is the vibrational distribution or the vibrational temperature? How rapidly a distribution is established? What are the roles of various processes in the establishment of a vibrational temperature? What is the rate of the molecular dissociation via the vibrational ladder? How does this rate compare with the direct plasma electron dissociation of the molecule?

Vibrational relaxation studies are numerous[1-3] with the main interest focoused on the effects of the V-T and V-V transitions on the relaxation times in different gases and gaseous mixtures. The effects of the V-V transitions on the molecular dissociation has also been considered[3], and a study[4] of the relaxation and dissociation in H_2 with the combined effects of e-V, V-T and V-

Manuscript approved March 20, 1984.

V processes has been performed. No detailed studies for such relaxations has been made in N_2 and air, however, some results for air have been reported[5].

In this paper we present a detailed study of the relaxation and dissociation of N_2 and attempt to answer the various questions raised earlier. We do this by solving a master equation described in Section II where e-V, V-T and V-V transitions are considered with different electron and gas temperatures. The appropriate rate coefficients, for the processes included in the master equation, are discussed in Section III, and the results of the calculations are presented in Section IV.

2. BASIC EQUATIONS

We consider the nitrogen molecule as a harmonic oscillator with a vibrational energy spacing[6] of ~ 0.30 eV and solve for the time development of 32 vibrational levels where the last level gives the density of the dissociated molecules. The processes that control the time histories of the vibrational levels are:

(a) The excitation and de-excitation of the vibrational level by electron impact, i.e.

$$e + N_2(v) \rightleftarrows N_2(w) + e \qquad (1)$$

Here, $N_2(v)$ indicates the population density of level v.

(b) The excitation and de-excitation of the vibrational level by collisions with molecules resulting in the vibrational-translation energy exchange, i.e. V-T transitions.

$$N_2(v) + M \rightleftarrows N_2(v+1) + M \qquad (2)$$

Where M is the total density of the molecules.

(c) The vibrational-vibrational transitions, i.e.

$$N_2(v) + N_2(w) \rightleftarrows N_2(v+1) + N_2(w-1) \qquad (3)$$

Where only a single vibrational quantum is exchanged.

The master equation which governs the population density of each vibrational level, except for level 32, is

$$\begin{aligned}\frac{dN_2(v)}{dt} &= \sum_{w=1} N_{v+1} N_{w-1} P^{w-1,w}_{v+1,v} - \sum_{w=1} N_v N_w P^{w,w-1}_{v,v+1} \\ &- \sum_{w=0} N_v N_w P^{w,w+1}_{v,v-1} + \sum_{w=0} N_{v-1} N_{w+1} P^{w+1,w}_{v-1,v} \\ &+ \sum_w N_e N_w X_{wv} - \sum_w N_e N_v Y_{vw} \\ &- \sum_v N_v M R_{v,v+1} + \sum_w N_w M S_{w,w-1}\end{aligned} \qquad (4)$$

Here $P^{w-1,w}_{v+1,v}$ indicates the rate coefficient for the vibrational-vibrational energy exchange, i.e, the V-V transitions. Under this process a molecule at the (v+1) level loses one vibrational quantum and descsends to level v while the molecule at the (w-1) vibrational level gains the vibrational quantum and

ascends to level w. The electron impact excitation resulting in the molecular transition from level w to v is indicated by X_{wv}. The corresponding de-excitation rate is given by Y_{vw}. On the other hand, the rate coefficient for the vibrational translational-collisions, i.e. V-T transitions, resulting in a vibrational excitation is represented by $R_{v,v+1}$ and the corresponding reverse process is indicated by $S_{w,w-1}$.

The equation that describes the population density of level 32 is similar to Eq. 4 with the condition that the inverse processes which depopulate level 32 are not allowed.

3. RATE COEFFICIENTS

The electron impact rate coefficient for the vibrational excitation is obtained from the measured cross sections[7,8]. These cross sections for transitions from v=o to v=8 have been averaged[9] with the electron velocity over a Maxwellian electron velocity distribution and the rate coefficients are shown in Fig. 1.

For electron impact excitations to levels above v=8 we utilize the following often used[4] relation,

$$X_{v,\ v+\Delta v} = X_{o,\ \Delta v} \tag{5}$$

The electron impact de-excitation rate coefficient, $Y_{v,w}$ is obtained from the corresponding excitation rate by the principle of the detailed balance, i.e.,

$$Y_{v,w} = X_{w,v}\ \mathrm{Exp}\ [-\ 0.3\ (v-w)/T_e] \tag{6}$$

where T_e is the electron temperature in eV.

The vibrational-translational rate coefficients $S_{w,w-1}$ is obtained from the de-excitation rate of v=1 state, S_{10}, and the harmonic oscillator relation i.e.

$$S_{v+\Delta v,v} = (v+\Delta v)\, S_{10} \tag{7}$$

where[10]

$$S_{10} = 8.5 \times 10^{-7}\ \mathrm{Exp}\ \left(-\frac{12.4}{(T_g)^{1/3}}\right) \tag{8}$$

Here T_g is the gas temperature in units of eV. It should be noted that relation (8) is valid for the temperature range of T_g=0.086 eV to 0.43 eV On the other hand, for V-T excitations, one has

$$R_{v,v+\Delta v} = (v+\Delta v)\, S_{01} \tag{9}$$

and S_{01} is related to S_{10} by the detailed balance.

The V-V transition rate coefficients are obtained by using the probability of energy exchange per collision derived by Rapp and Englander-Golden[11]. This probability is

$$A^{rn}_{sm} = \mathrm{Sin}^2(4\,\pi\,\mu\, L V_o\, U_{rn}\, U_{sm}/h)\ \mathrm{Sech}^2\left(\frac{2LE_d}{V_o}\right) \tag{10}$$

where μ is the reduced mass, L is a characteristic length which enters the exponential of the repulsive potential, V_o is the velocity of the colliding particle, U_{rn} is the matrix element for transition between states r and n and E_d is the energy defect. We shall consider the case of a harmonic oscillator with E_d=o. The Sin^2 term in Eq. (10) can be approximated by the square of the argument as shown by Fisher and Kummler[2]. With these assumptions, the probability per collison for transitions from v=1 to v=o can be written as

$$A_{01}^{10} = 16\pi^2\mu^2L^2(U_{01})^4 \frac{V_o^2}{h^2} \tag{11}$$

The matrix element for a harmonic oscillator[3] is

$$(U_{01})^2 = (\frac{1}{4L})^2 \frac{h}{\pi M\nu} \tag{12}$$

Where M is the mass of an atom and ν is the vibrational frequency. Substituting Eq. (12) into (11) and using[2] L = 0.2Å we obtain

$$A_{01}^{10} = 4.0 \times 10^{-2}\ T_g \tag{13}$$

Where T_g is in eV. The rate coefficient for V-V transitions is obtained by multiplying the probability for energy enchange by the collision rate

coefficient i.e. σV_o . Where σ is the cross section for hard sphere collisions and V_o is the average velocity. Using a value[12] of 3.75Å for the diameter of the nitrogen molecule, equation (13), and the average velocity as a function of gas temperature we obtain the necessary rate coefficent.

$$P_{01}^{10} = A_{01}^{10} \sigma V_o = 5.0 \times 10^{-11} (T_g)^{3/2} \tag{14}$$

Hence, the V-V transition rates for arbitrary levels, using harmonic oscillator relations[3], are

$$P_{v+1,v}^{w-1,w} = (v+1)w \; P_{10}^{01}$$

and (15)

$$P_{v,v+1}^{w,w-1} = w(v+1) \; P_{10}^{01}$$

4. RESULTS AND ANALYSIS

The master equation discussed in Section II is solved for v = 0 to v = 32 and as a function of time using a computer. The solutions are carried out for a range of electron densities from $10^{12}cm^{-3}$ to $10^{15}cm^{-3}$ in a 640 Torr of nitrogen. The electron and gas temperatures were different and assumed to have Maxwellian distributions. Three gas temperatures of 0.025eV, 0.25eV and 0.5eV were chosen with electron temperatures of 1.0eV. The results are discussed below.

4.1 THE VIBRATIONAL RELAXATION AT T_g = 0.025eV

Figures 2-5 show typical results depicting the population densities of 13 vibrational levels of v = 0 to v = 12 as a function of time for the initial conditions of $N_2(0) = 2.1 \times 10^{19}cm^{-3}$, $N_e(10^{12}cm^{-3} - 10^{15}cm^{-3})$, T_e = 1.0 eV and T_g = 0.025eV. These figures show that the vibrational levels attain a quasi-steady state distribution which signifies the development of a vibrational temperature. The establishment of the vibrational distrubution clearly depends on various parameters which determine how fast such a distribution takes place. For example in Figures 2-5 the electron density is varied from $10^{12}cm^{-3}$ to $10^{15}cm^{-3}$, while the rest of the parameters i.e. the electron and gas temperatures are kept the same. We observe that the vibrational distribution is established in a time, τ_v , which becomes shorter the higher the electron density. This time for $n_e = 10^{12}cm^{-3}$, $10^{13}cm^{-3}$, $10^{14}cm^{-3}$ and $10^{15}cm^{-3}$ is 2×10^{-4} sec, 2×10^{-5}sec, 2×10^{-6}sec and 2×10^{-7}sec, respectively. Under these conditions, the e-V collisions controls the time for the establishment of the vibrational distribution, because at room temperature the V-V transition rates are very small especially for the lower vibrational levels whose population densities are controlled by electron impact. The vibrational distribution time τ_v reduced approximately an order of magnitude when the electron density is increased by an order of magnitude.

The vibrational distribution as calculated by the master equation can be characterized by a temperature T_v, where T_v is deifined by the usual harmonic oscillator relation for a Boltzman distribution i.e.

$$E_v = 0.3\ [Exp(\frac{0.3}{T_v})-1]^{-1} \qquad (16)$$

Here E_v is the average vibrational energy of the molecule and is obtained by the following relation

$$E_v = \frac{\sum_v 0.3\ v\ N_2(v)}{\sum_v N_2(v)} \tag{17}$$

Under the conditions where the T-V and V-V rates are negligible we observe that the vibrational temperature is controlled by electron molecule collisions and that the vibrational temperature, as defined above, approaches the electron temperature as shown in Figure 6. The vibrational temperature becomes closer to the electron temperature for higher electron densities. The calculated densities of the vibrational levels are in Boltzmann equilibrium for the mid vibrational levels, slightly higher than Boltzmann for the lower levels and underpopulated for levels closer to the dissociation limit. This under population is partially due to the neglect of the three-body neutral recombination to different vibrational levels and partially to the ease of dissociation from such high levels.

The population density of level 32, i.e., the number of molecules dissociated, is shown in Figure 7 as a function of time for the same range in the electron density ($10^{12}cm^{-3}$ - $10^{15}cm^{-3}$). An obvious feature in Figure 7 is that the higher the electron density the faster is the molecular dissociation. This is due to enhanced collision rates with increased electron density.

4.2 THE VIBRATIONAL RELAXATION AT ELEVATED GAS TEMPERATURE

In this section we present the relaxation calculations for two nitrogen

gas tempertures of 0.25eV and 0.50eV where the effects of V-T and V-V can be seen more effectively.

Figures 8-11 show the population densities of thirteen vibrational levels v=0 to v=12 for T_g = 0.25eV and electron densities of $10^{12}cm^{-3}$ to $10^{15}cm^{-3}$. The vibrational distribution is developed in time scales of 10^{-4}sec, $2x10^{-5}$ sec, $2x10^{-6}$sec and $2x10^{-7}$ for N_e = $10^{12}cm^{-3}$, $10^{13}cm^{-3}$, $10^{14}cm^{-3}$ and $10^{15}cm^{-3}$, respectively. These times are not different from those presented in Section 4.1 for T_g = 0.025eV indicating that electron-molecule collisions and V-V transitions are still dominant in establishing the vibrational equilibrium. The vibrational temperatures for these distributions are shown in Figure 12. It is interesting to observe that these temperatures are lower for each electron density compared with those shown in Figure 6. Thus the T-V and V-V processes apparently depress the vibrational temperature compared to the temperature obtained from purely e-V processes. This is because the de-excitation rates for T-V and V-V are larger than the corresponding rates at T_g = 0.025 eV. Furthermore, the vibrational levels are in near Blotzmann distribution for the lower and mid levels while the levels near the dissociation limit are underpopulated compared to Boltzmann relation at the derived temperature.

At a gas temperature of 0.5eV, the results are much different than those at T_g = 0.25 eV. For example, the vibrational distribution is established at times of $2x10^{-6}$sec, $3x10^{-6}$sec, $7x10^{-7}$sec and $2x10^{-7}$sec for n_e=$10^{12}cm^{-3}$, $10^{13}cm^{-3}$, $10^{14}cm^{-3}$, and $10^{15}cm^{-3}$ respectively as shown in Figures 13-16. These times are much shorter compared to those obtained at lower gas temperature, especially for lower electron densities which implies that V-T and V-V are now comparable and even higher than the e-V rates for lower electron densities. The vibrational temperatures, obtained with Eqs. 16 and

17 which characterize the development of the vibrational distributions are shown in Figure 17. Again, the vibrational temperatures are lower compared to those for lower gas temperatures. The level populations near the dissociation limit as before, are underpopulated compared to a Boltzmann distribution at the calculated T_v. The mid level populations are near Blotzmann and the lower levels are slightly overpopulated.

4.3 THE T-V AND V-V EFFECTS ON THE VIBRATIONAL DISTRIBUTION FOR A FIXED N_e

For an electron density of $10^{12}cm^{-3}$, the case of low electron density, the evolution of the vibrational temperature for three gas temperatures is shown in Figure 18. The following observation can be made; (a) the vibrational distribution is established faster for higher gas temperatures because of the enhanced V-V and T-V rates (b) the vibrational temperature is lower for higher gas temperatures because V-V and T-V processes tend to depress the vibrational level populations (c) the gas temperature effects are different depending on whether T_g is low or high. For example, at T_g=0.25eV the vibrational temperature is depressed more compared to that for T_g=0.5eV. This is because the V-T deexcitation rates are not compensated by the inverse excitation processes.

4.4 THE DISSOCIATION RATE

In the computer solution of the master equation, level 32 designated the number of molecules dissociated under the total actions of e-V, V-V and V-T processes. An overall dissociation rate under these conditions can be obtained by defining the dissociation rate, K_d, in the following manner

$$K_d = \frac{dN_2(32)/dt}{\sum_v N_2(v)} \qquad (18)$$

This expression slightly over estimates the dissociation rate since we do not account for the three body atomic recombination into molecules. Figure 19 shows the dissociation rate using Eq. 18 for $N_e = 10^{12}$ and three gas temperatures. The quasi steady state dissociation rates represented by the plateaus in Figure 19 show a very interesting result. The dissociation rate for the gas at the room temperature is higher than the dissociation rate when $T_g > 0.025$ eV. On the other hand, the dissociation rate when $T_g = 0.25$eV is lower than when T_g is 0.5eV. To understand this behaviour one can look at the vibrational temperature under these conditions (see Figure 20) where for higher dissociation rates one also has higher vibrational temperatures. This implies that the higher vibrational states are highly populated which then are easily dissociated. To further understand the contributions of various processes to the overall dissociation rate consider for example Figure 21. In this Figure, we see that for $T_g = 0.5$eV the dissociation rate, when all physical processes are included, is given by graph (a) and indicates a value of 40 sec^{-1}. However, when one turns off the e-V processes, the dissociation rate, given by graph (b), is practically unchanged compared to graph (a). This implies that for low electron density (in this case $N_e = 10^{12} cm^{-3}$), the V-V and T-V processes dominate at $T_g = 0.5$eV. When we turn off the T-V processes, the dissociation rate is the highest with a value of 400 sec^{-1} and is indicated by graph (c) which implies that V-V processes contribute predominately to the dissociation. On the other hand, when we turn off the

V-V processes the dissociation rate given by graph (d) indicates a value of $2.5 \times 10^{-1}sec^{-1}$ which is much smaller than the previous rates discussed above. Finally when we turn off both V-V and T-V processes we obtain a dissociation rate of $\sim 4.5 \times 10^{-1}sec^{-1}$, indicated by graph (e). This implies that at an electron temperature of 1.0eV and a gas temperature of 0.5eV the dissociation rate due to electron molecule collisions alone is equal to the dissociation rate due to T-V processes with one exception, that is, the establishment of the vibrational distribution and the molecular dissociation occurs much faster with V-T transitions compared to that with only e-V processes (see Figure 22).

However, the dissociation rates for electron densities higher than $10^{12}cm^{-3}$ are shown in Figures 23 and 24. Where for $N_e = 10^{13}cm^{-3}$ we observe the rate of dissociation at T_g = 0.25 eV to be below that for T_g = 0.025 but very close to it while for $N_e = 10^{14}cm^{-3}$ the dissociation rate for T_g = 0.25eV exceeds that for T_g = 0.025eV. In general, the higher the vibrational temperature the higher is the dissociation rate as can be seen in Figures 25 and 26. One exception here is the higher dissociation rate for T_g = 0.25 compared to that for T_g = 0.025 at an electron density of $10^{14}cm^{-3}$ where the vibrational temperature is higher for T_g = 0.025 compared to that for T_g = 0.25 (see Fig. 26). The physical explanation for this is that the higher vibrational levels near the dissociation limit are affected drastically by T-V and V-V processes which are generally depressing in nature i.e., they tend to relax the levels downwards. This downward trend is more than offset by the large rate of electron molecule collisions for $N_e = 10^{14}cm^{-3}$ while at T_g = 0.25 these two processes barely compensate each other because of increased VT rates.

Finally, it is of interest to show that the vibrational levels will start

to decay with increased dissociation beyond the steady state. This situation is demonstrated in a typical example in Figure 27.

5. ELECTRON IMPACT DISSOCIATION OF N_2

The electron impact dissociation of nitrogen has been measured by Winters[13]. More recently however, Zipf and McLaughlin[14] have performed a more comprehensive study of the electron impact dissociation. This study has delineated the basic processes and the states that contribute to the dissociation. It is concluded that all singlet states (~ 54 states) of the $^1\pi$ and $^1\Sigma$ manifolds and in the energy range of 12.5 - 14.8 eV predissociate completely. Furthermore, the sum of the excitation cross sections for these states comprises 60% of the total dissociation cross section measured by Winters[13]. The rest of the dissociation arises as a result of excitation to levels higher than 14.8 eV.

The various inelastic electron impact scattering studies[1] on N_2 and the extreme ultraviolet absorption measurements[2] have indicated that nitrogen possesses a large number of singlet states in the range of 11.5 - 40 eV. These states are generally characterized as Valence and Rydberg like with life times in the range of 1 - 100 nsec. Hence it is expected that these states emit considerable amount of radiation in the extreme ultraviolet. However, because of the predissociation of these states the euv emission will be minimal. The reabsorption of these radiations also contributes to the dissociation of the molecule[14,17].

Thus the total dissociation cross section for N_2 as illustrated by Zipf and McLaughlin includes the contribution from states above 14.8 eV which includes dissociation leading to excited nitrogen atoms, states with 17.3 eV peak from Lassettre's data[15], Rydberg states, triplet states above 11 eV, and

part of the $a^1\pi_g$ state. The dissociation cross section for the optically thin and thick cases are obtained and are in good agreement with Winters' measurement[13]. These cross sections are averaged over a Maxwellian electron velocity distribution and the dissociation rates have been obtained[9,14]. From these one observes that the dissociation rate coefficient for electrons with T_e = 1.0 eV is 1.4×10^{-13} cm^3/sec. Accordingly, the dissociation rate due to this process alone is $1.4\times10^{-1} sec^{-1}$ for $N_e = 10^{12}$ cm^{-3} at room temperature compared to a rate of dissociation of 240 sec^{-1}(see Fig. 19) due to the vibrational ladder route as in the model discussed in the paper. For N_e = 10^{14} and $\bar{T}_g$ = 0.025 the corresponding rates are 14 sec^{-1} and 1500 sec^{-1}, respectively, indicating that the ladder climbing enhances the moleuclar dissociation.

In conclusion, we have provided a model for the molecular dissociation in a nitrogen discharge with a low degree of ionization where basic processes resulting in the dissociation are delineated. We plan to include the effect of an harmonicity to this model in the future. However, we are currently in the process of completing a new vibrational dissociation model due to the interaction of high energy electron beam with N_2 where the relevant temperatures are calculated from the first principles and are not held fixed as the model in this paper.

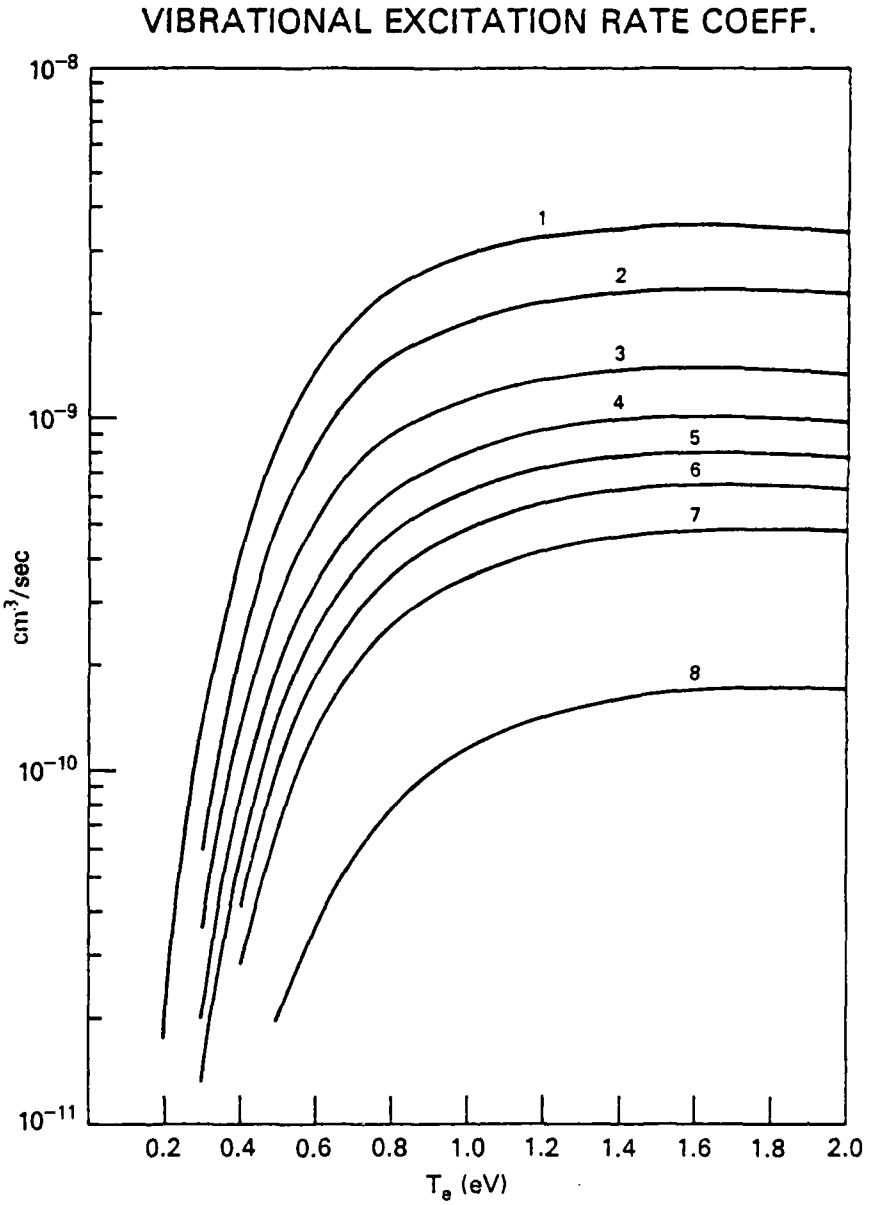

Fig. 1 Electron Impact Excitation Rate Coefficents for eight Nitrogen ground state vibrational levels

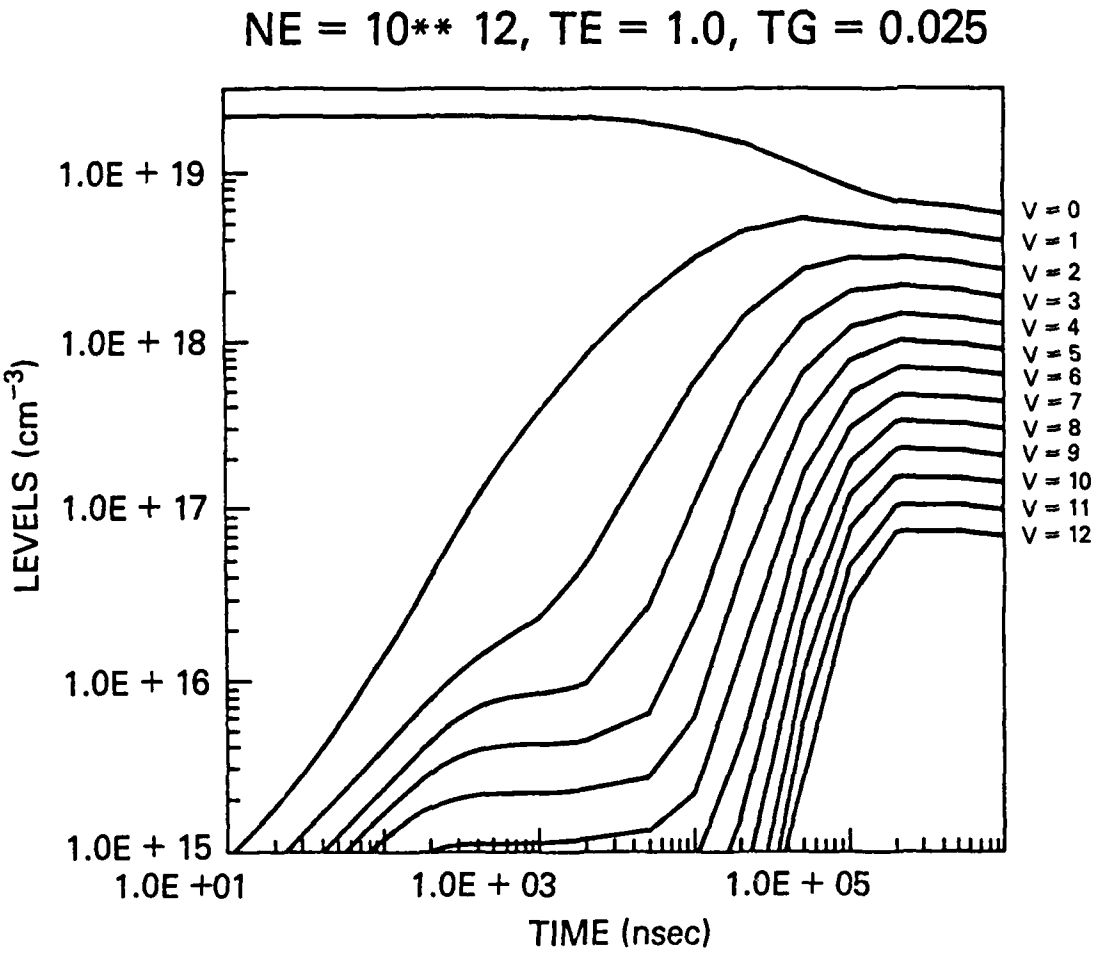

Fig. 2 Vibrational State Densities for $N_e = 10^{12} cm^{-3}$, T_e = 1.0 eV, and T_g = 0.025 eV

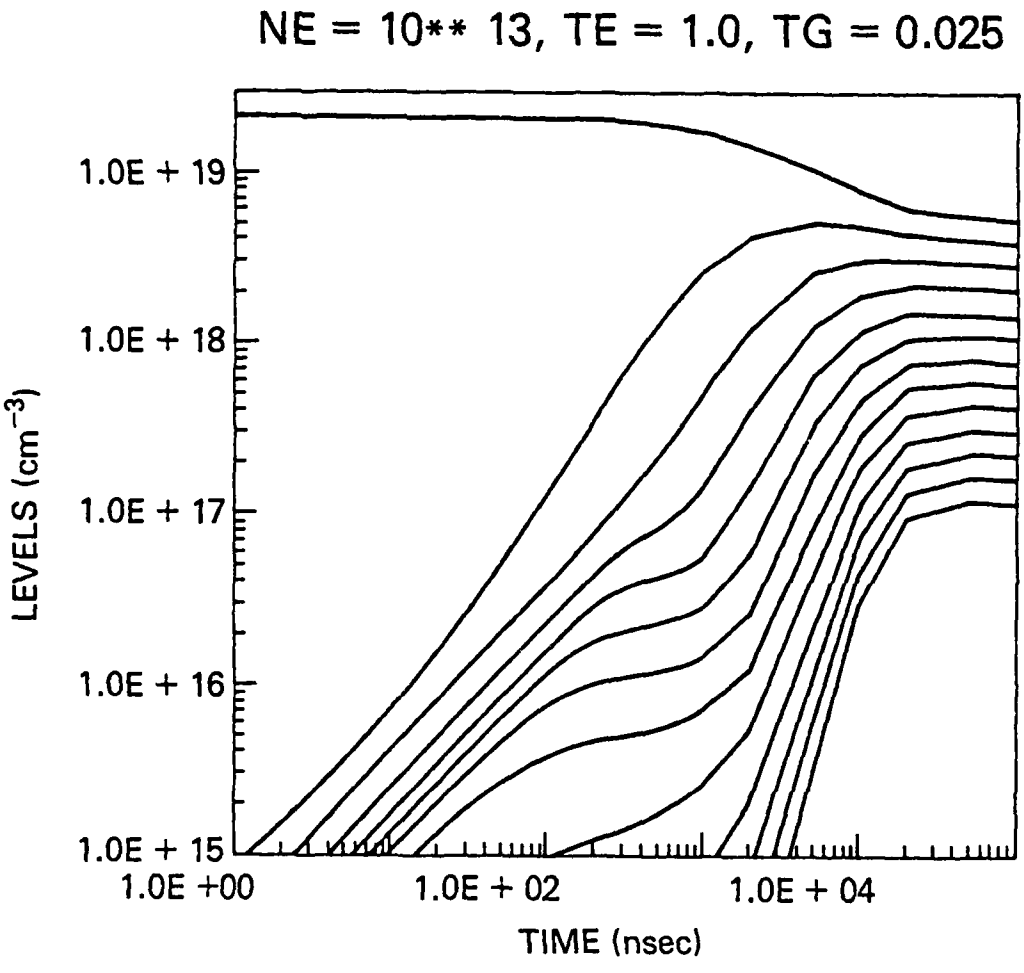

Fig. 3 Vibrational State Densities for $N_e = 10^{13}cm^{-3}$, $T_e = 1.0$ eV and $T_g = 0.025$ eV

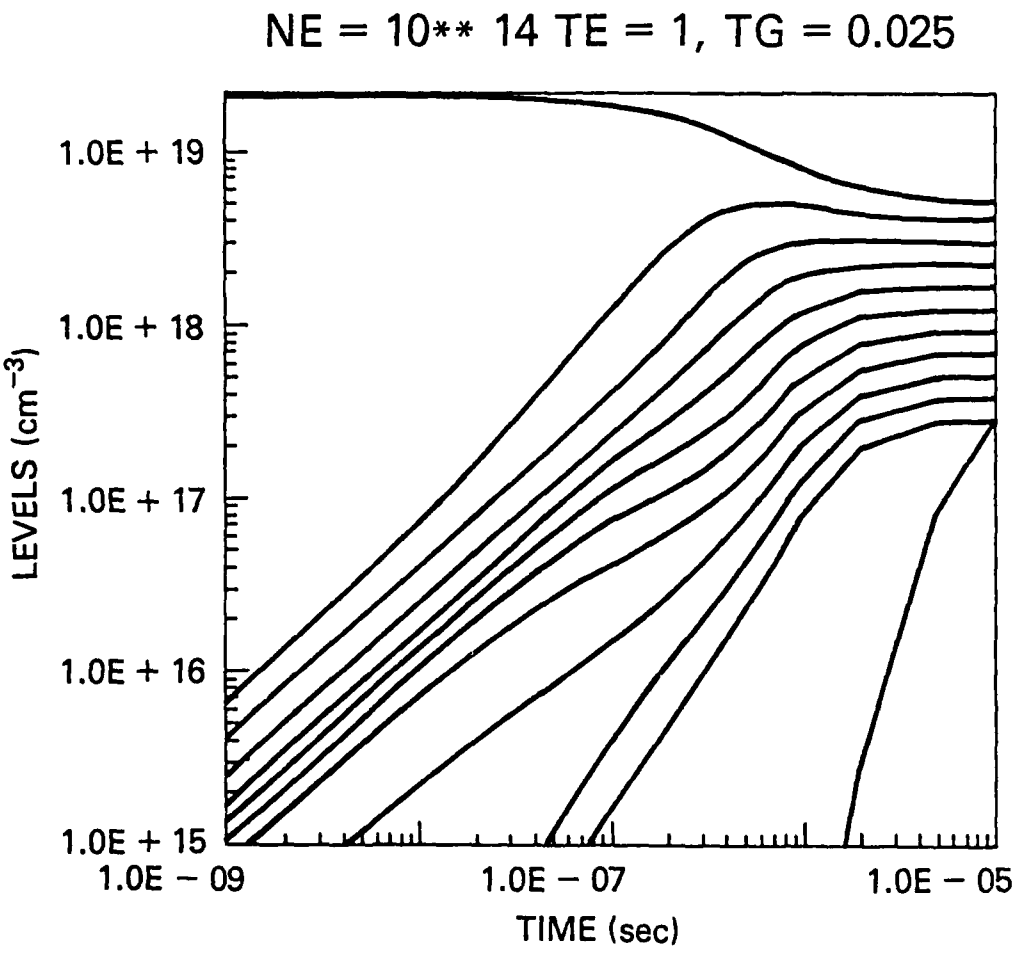

Fig. 4 Vibrational State Densities for $N_e = 10^{14} cm^{-3}$, T_e = 1.0 eV and T_g = 0.025 eV

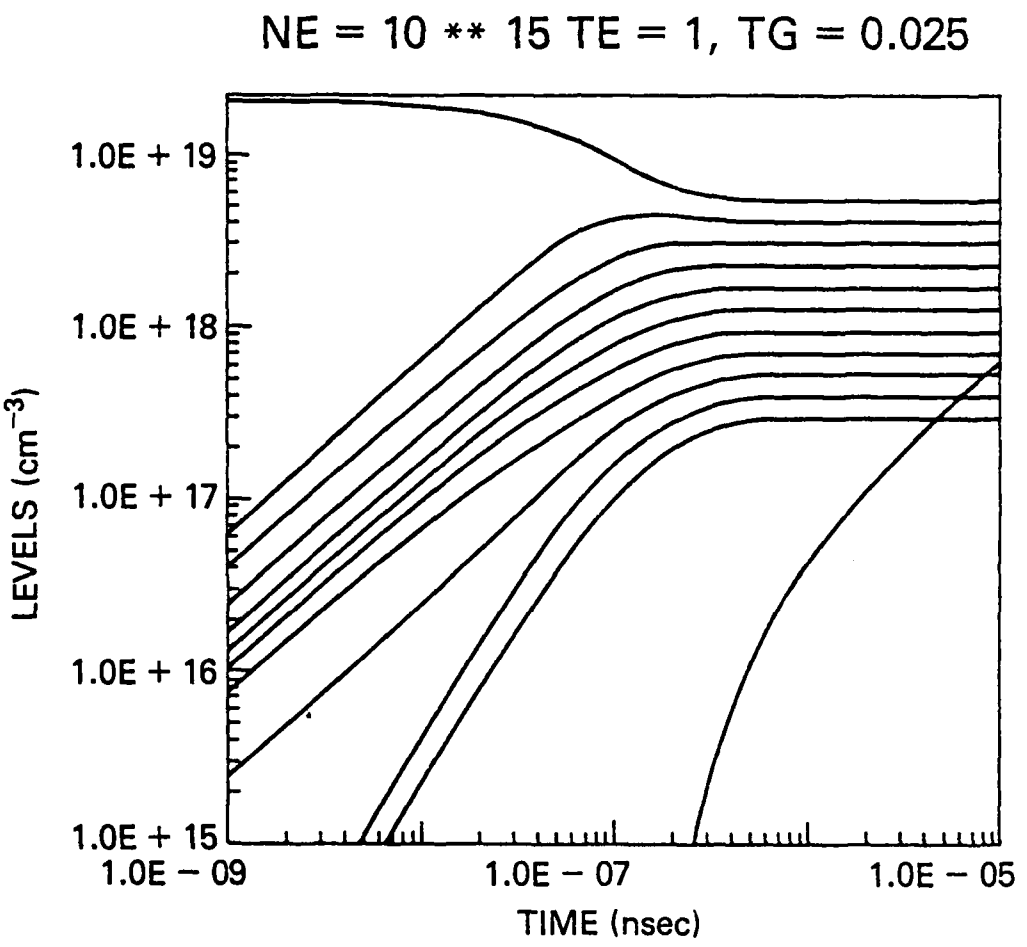

Fig. 5 Vibrational State Densities for $N_e = 10^{15} cm^{-3}$, T_e = 1.0 eV and T_g = 0.025 eV

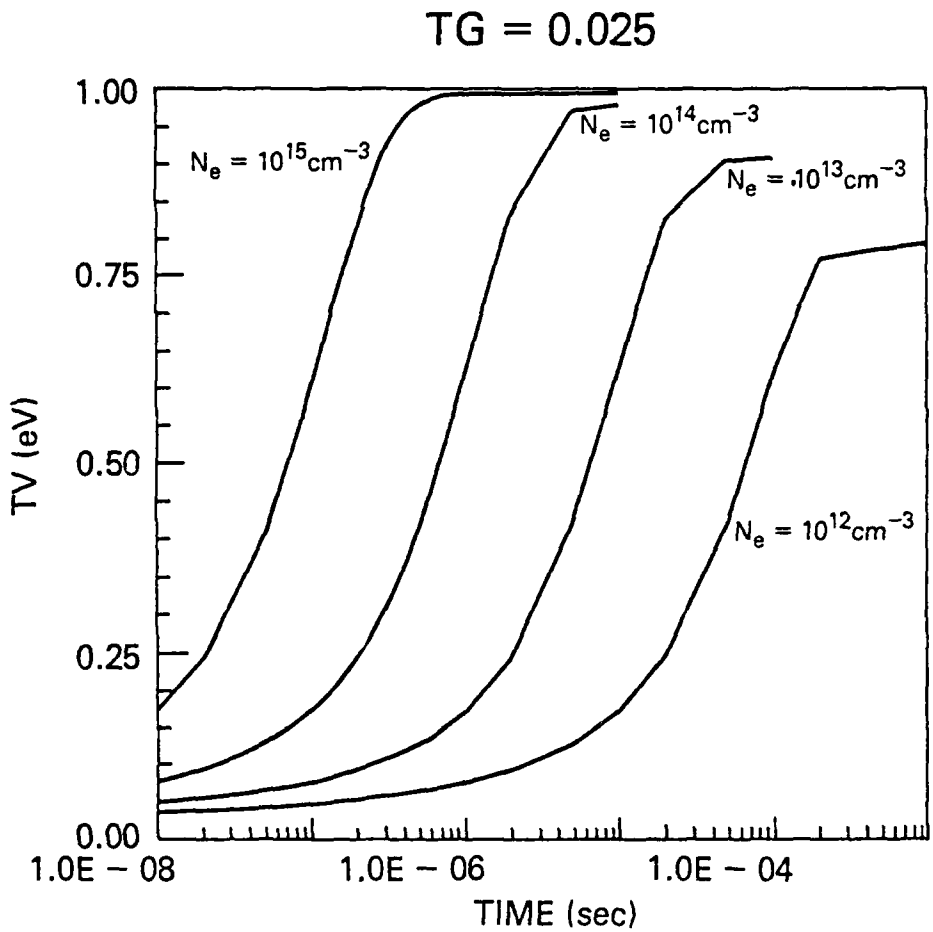

Fig. 6 The Vibrational Temperature for T_e = 1.0 eV, T_g = 0.025 eV and N_e = $10^{12}cm^{-3}$ - $10^{15}cm^{-3}$

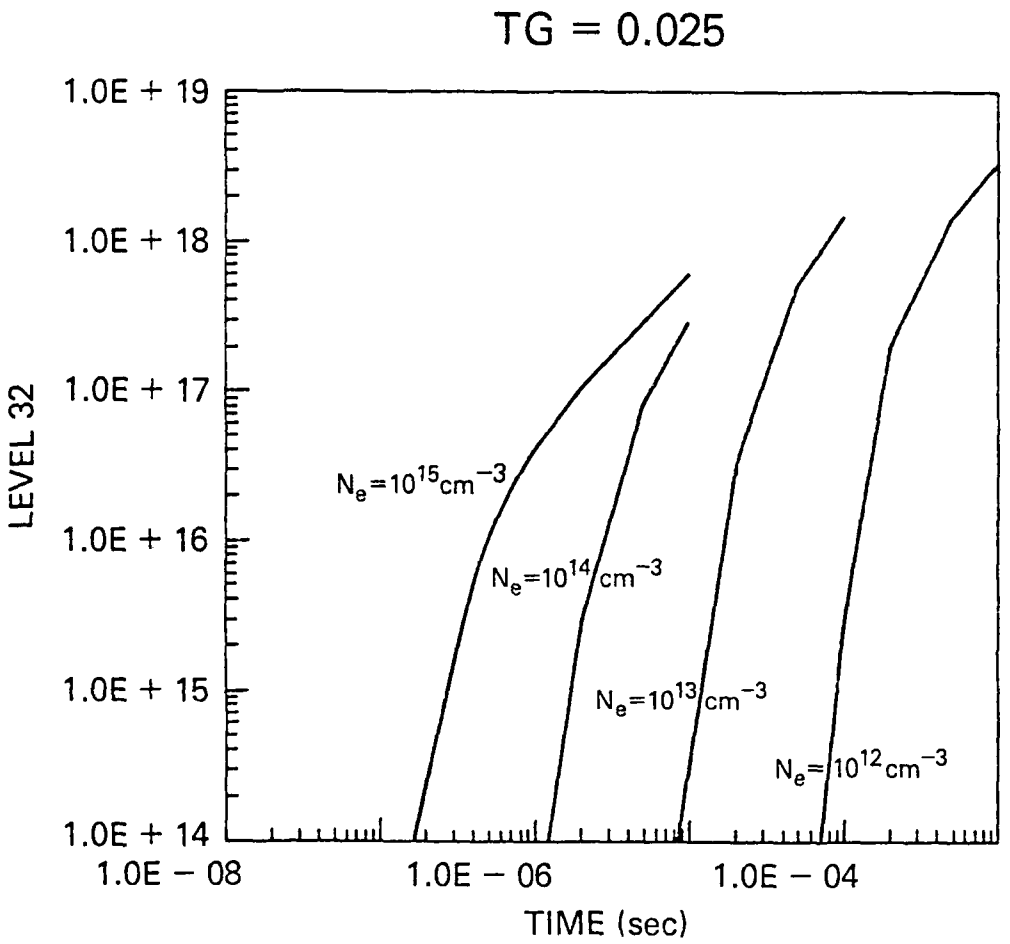

Fig. 7 Population Density of the Dissociated Molecules for T_e = 1.0 eV, T_g = 0.025 eV and N_e = $10^{12}cm^{-3}$ - $10^{15}cm^{-3}$

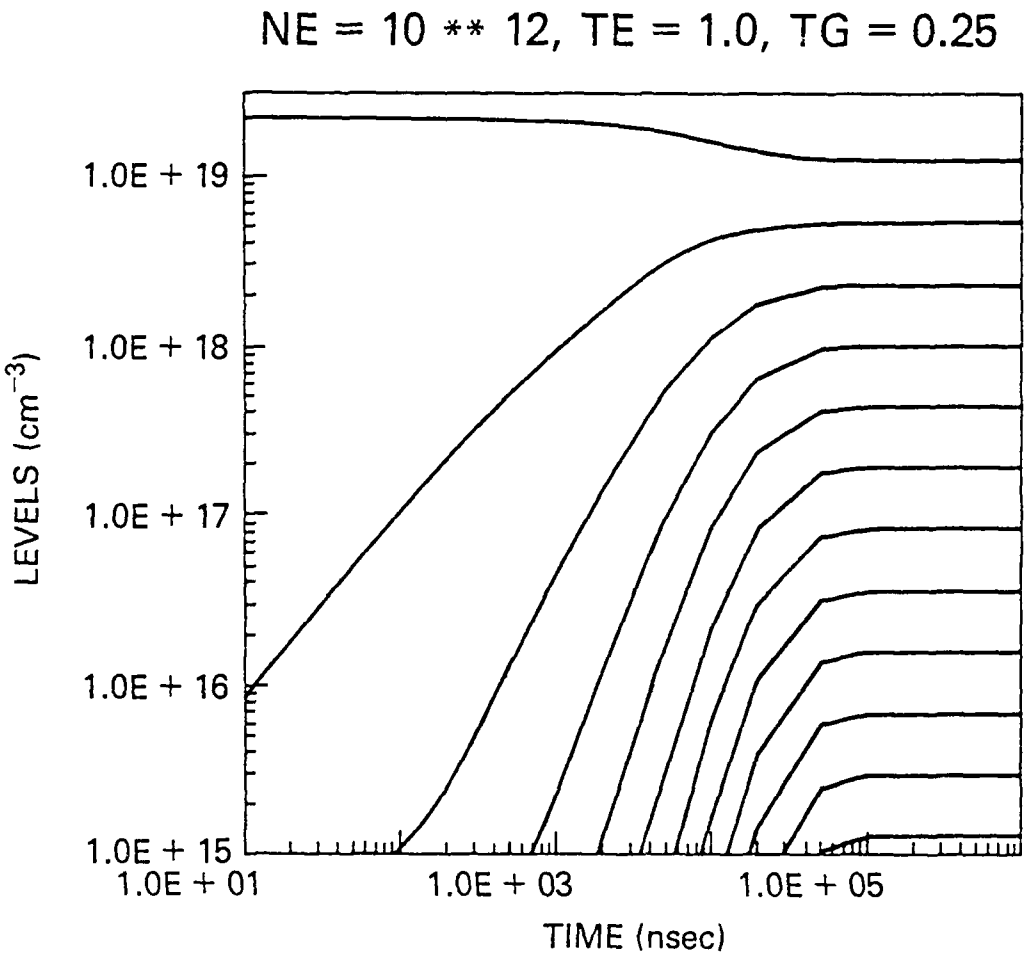

Fig. 8 Vibrational State Densities for $N_e = 10^{12} cm^{-3}$, $T_e = 1.0$ eV and $T_g = 0.25$ eV

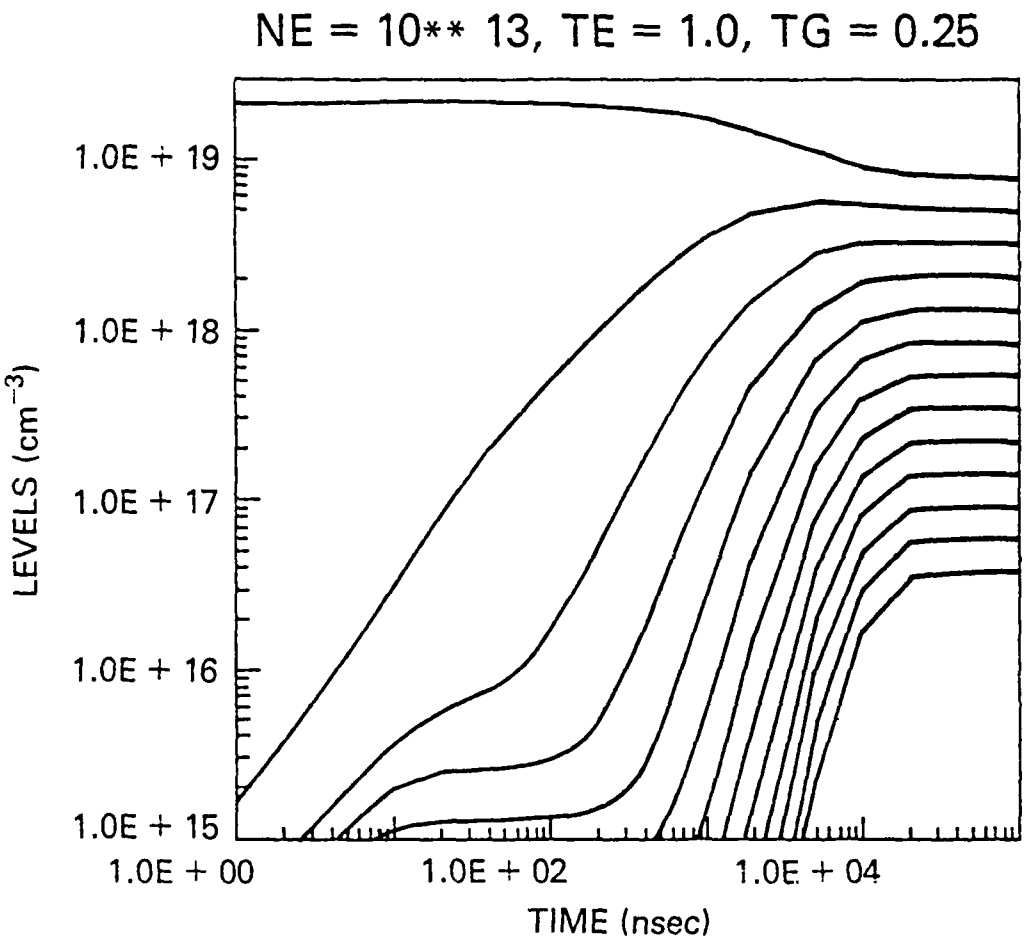

Fig. 9 Vibrational State densities for $N_e = 10^{13} cn^{-3} m$ T_e = 1.0 eV and T_g = 0.25 eV

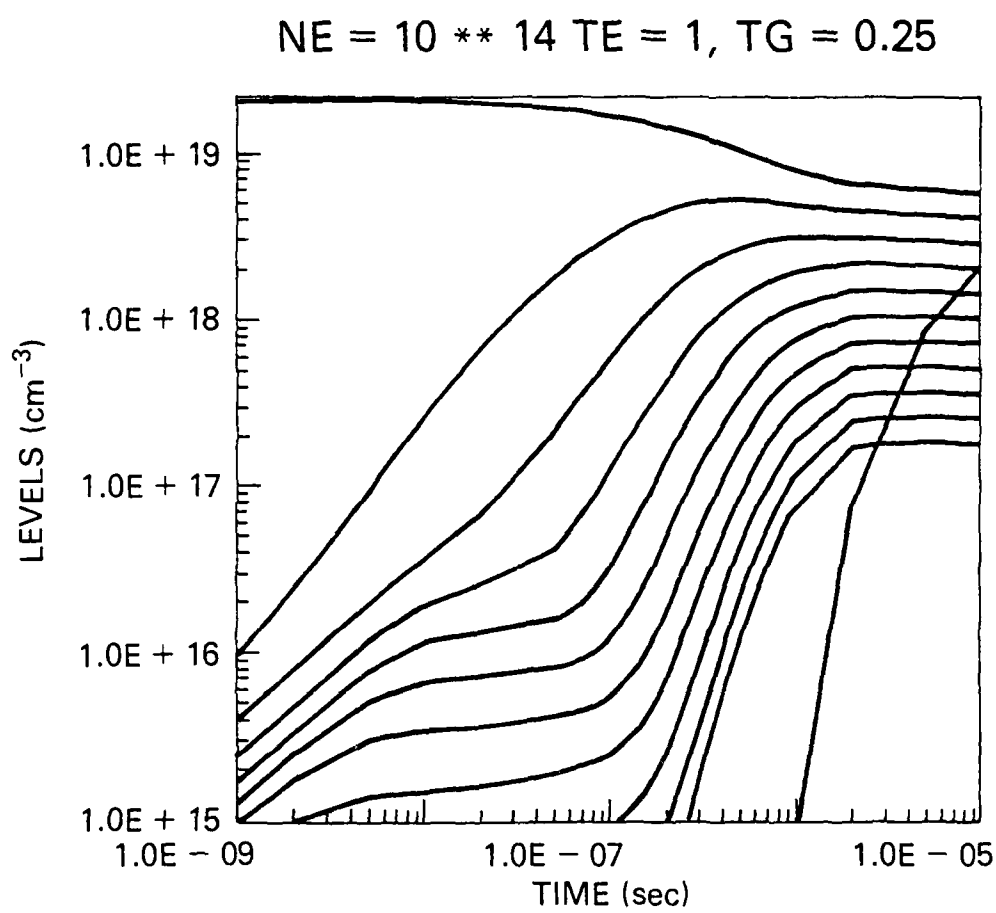

Fig. 10 Vibrational State Densities for $N_e = 10^{14} cm^{-3}$, T_e = 1.0 eV and T_g = 0.25 eV

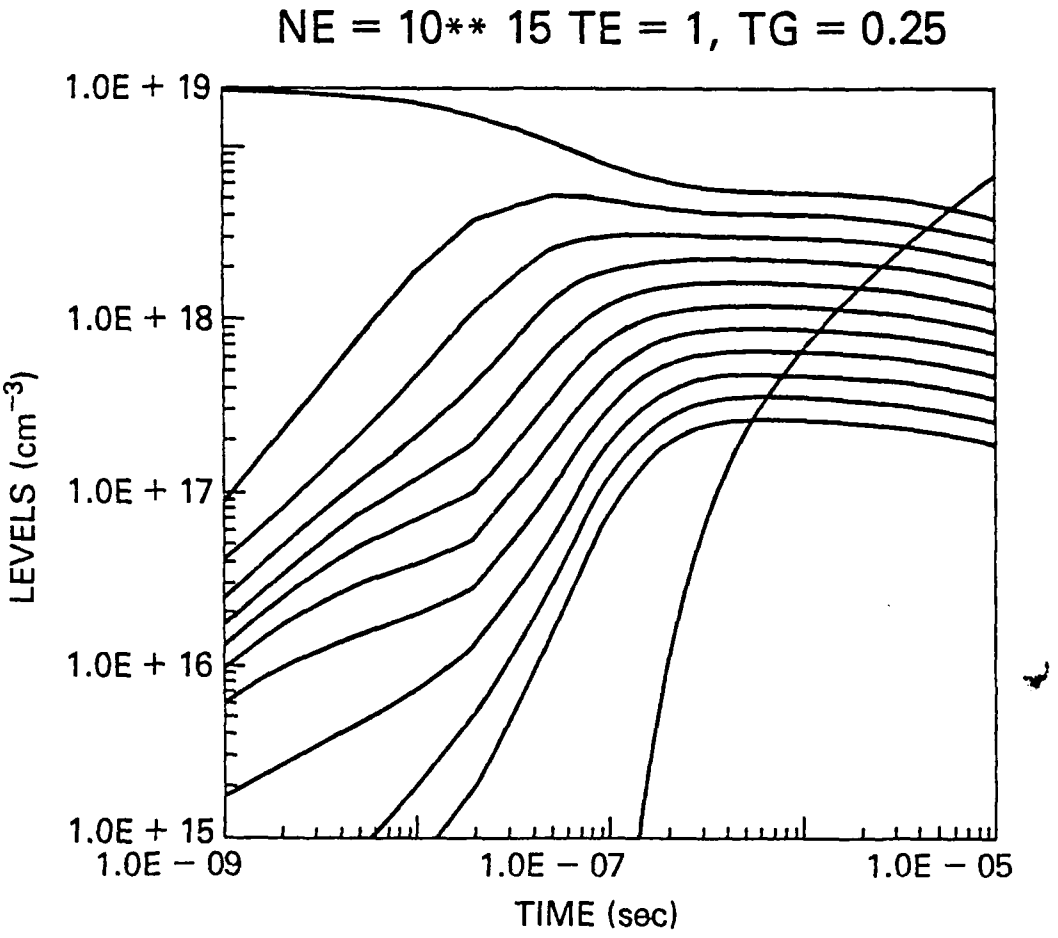

Fig. 11 Vibrational State Densities for $N_e = 10^{15} cm^{-3}$, T_e = 1.0 eV and T_g = 0.25 eV

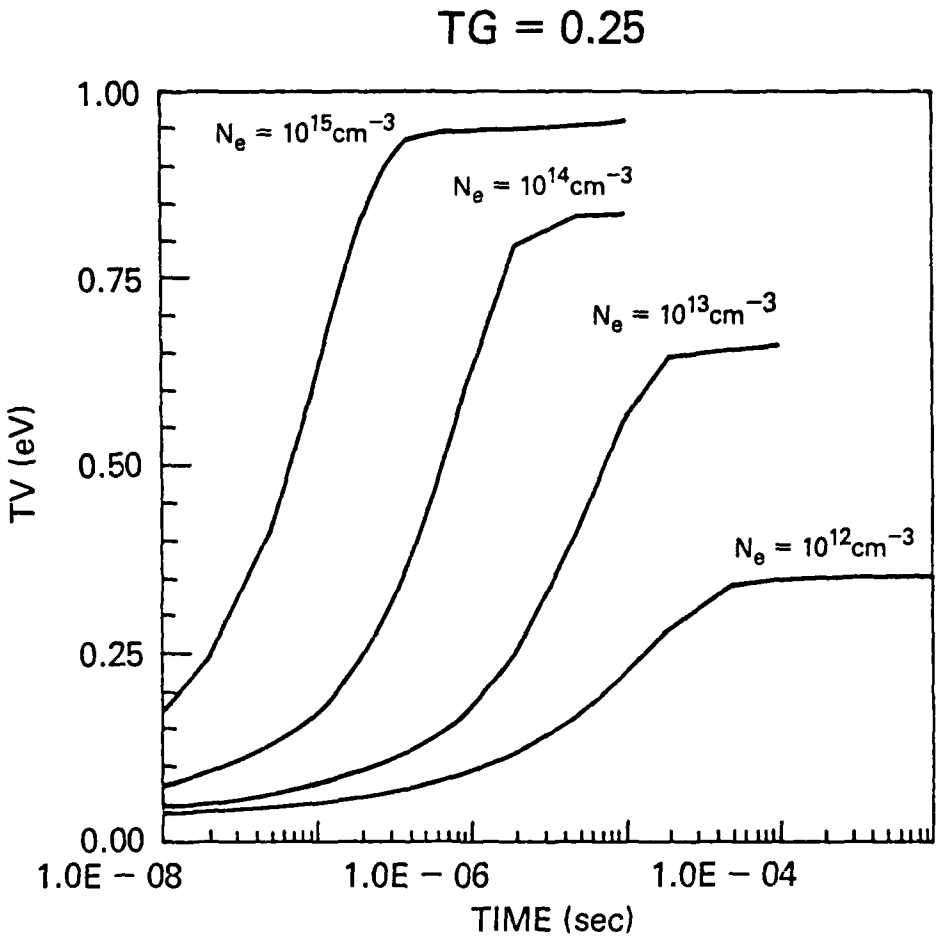

Fig. 12 The Vibrational Temperature for T_e = 1.0 eV, T_g = 0.25 eV and N_e = $10^{12}cm^{-3}$ - $10^{15}cm^{-3}$

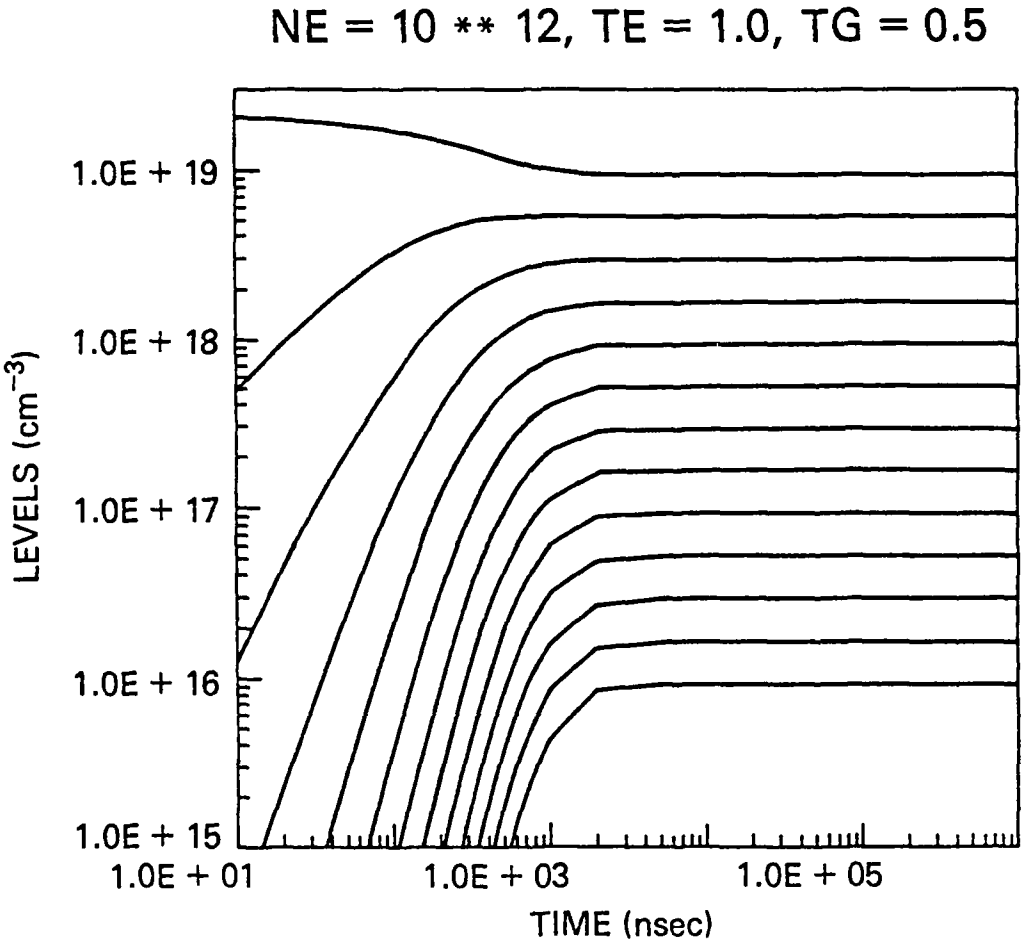

Fig. 13 Vibrational State Densities for $N_e = 10^{12} cm^{-3}$, T_e = 1.0 eV and T_g = 0.5 eV

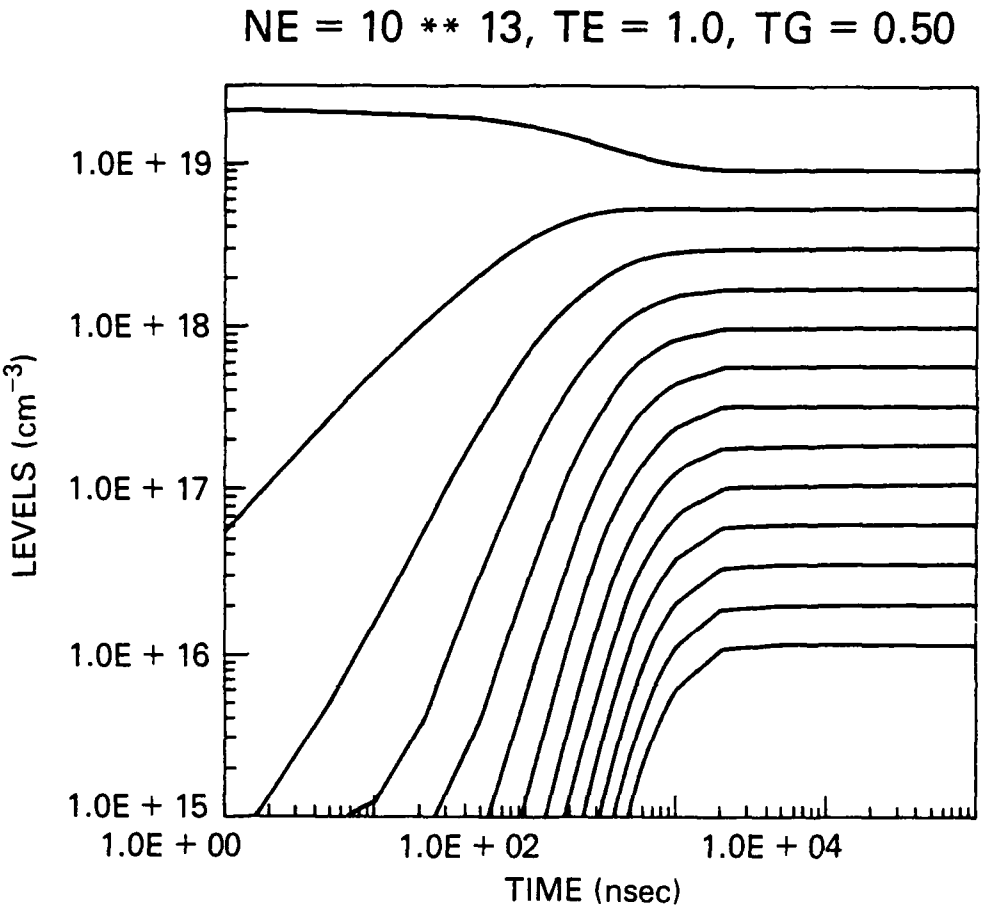

Fig. 14 Vibrational State Densities for $N_e = 10^{13} cm^{-3}$, T_e = 1.0 eV and T_g = 0.5 eV

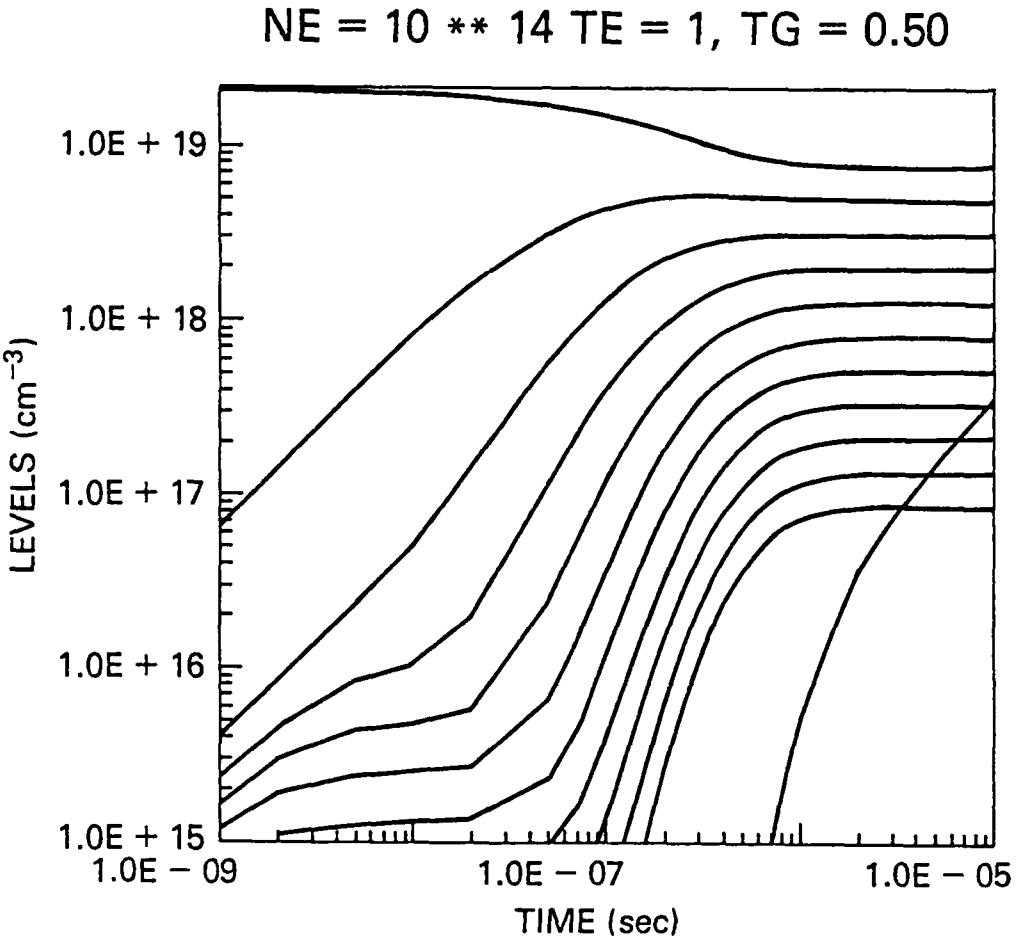

Fig. 15 Vibrational State Densities for $N_e = 10^{14} cm^{-3}$, T_e = 1.0 eV and T_g = 0.5 eV

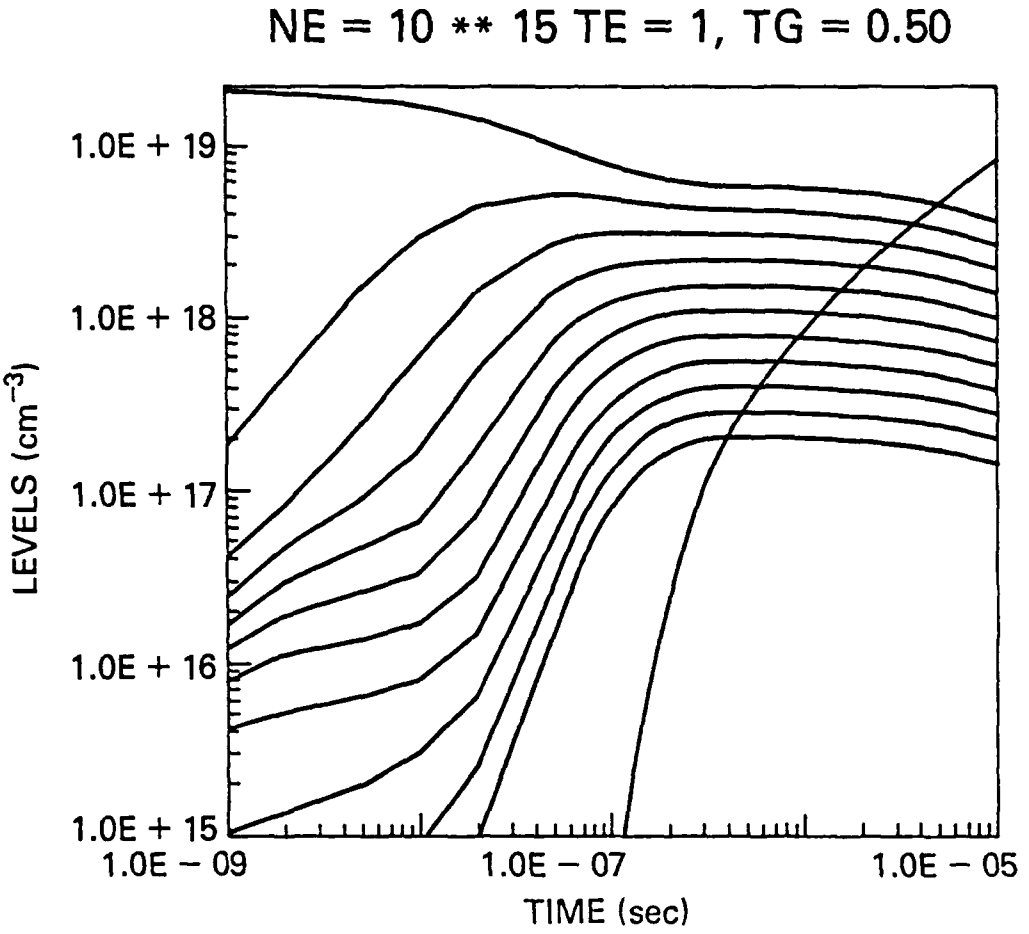

Fig. 16 Vibrational State Densities for $N_e = 10^{15} cm^{-3}$, T_e = 1.0 eV and T_g = 0.5 eV

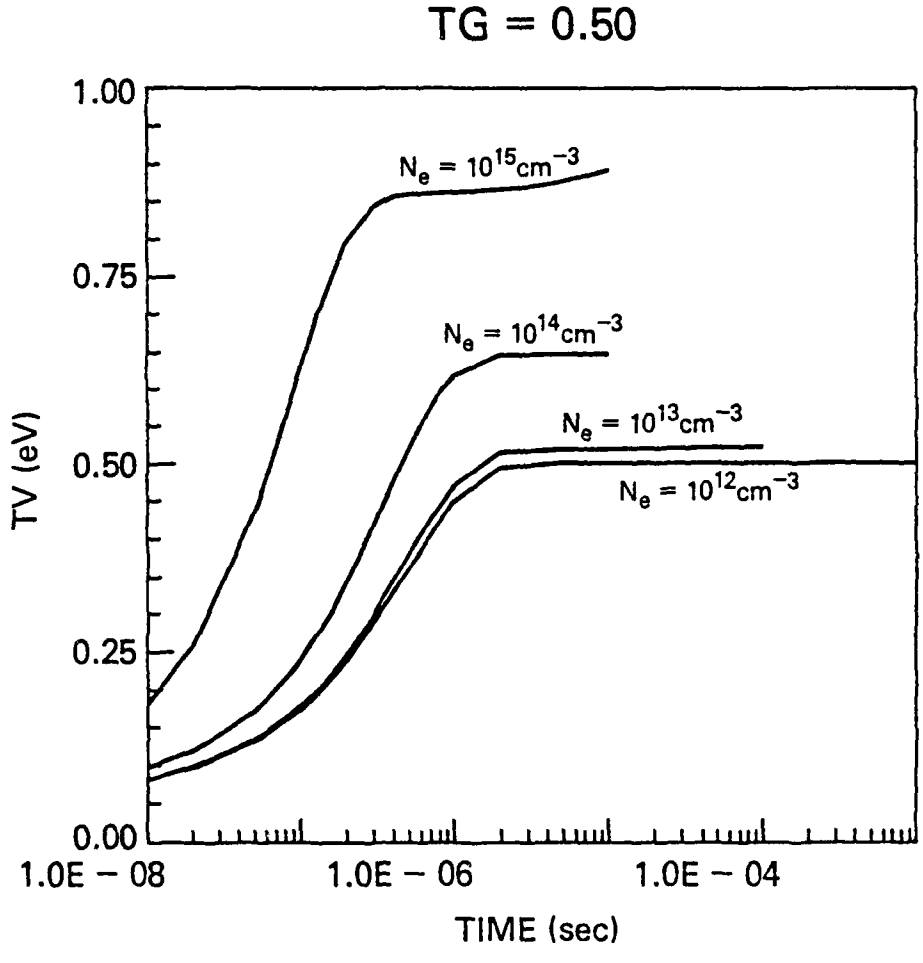

Fig. 17 The Vibrational Temperature for T_e = 1.0 eV, T_g = 0.5 eV and N_e = $10^{12}cm^{-3}$ = $10^{15}cm^{-3}$

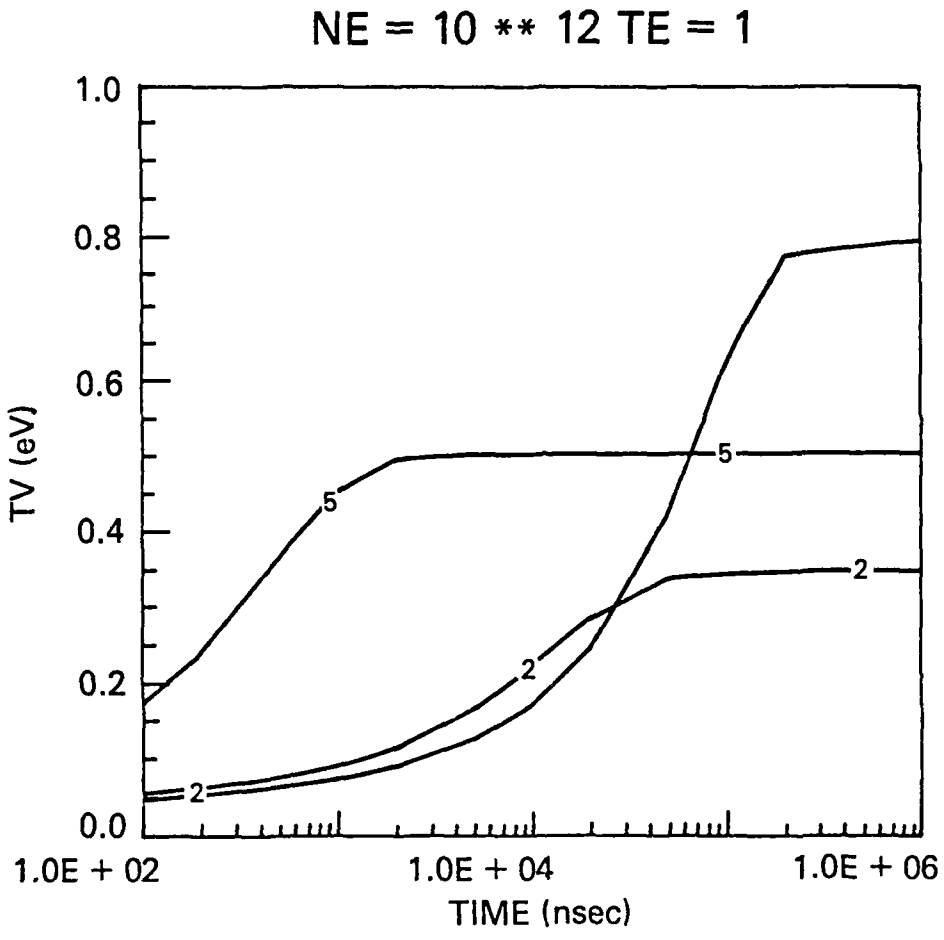

Fig. 18 The Vibrational Temperature for $N_e = 10^{12}cm^{-3}$, T_e = 1.0 eV and T_g = 0.025 eV, 0.25 eV and 0.5 eV

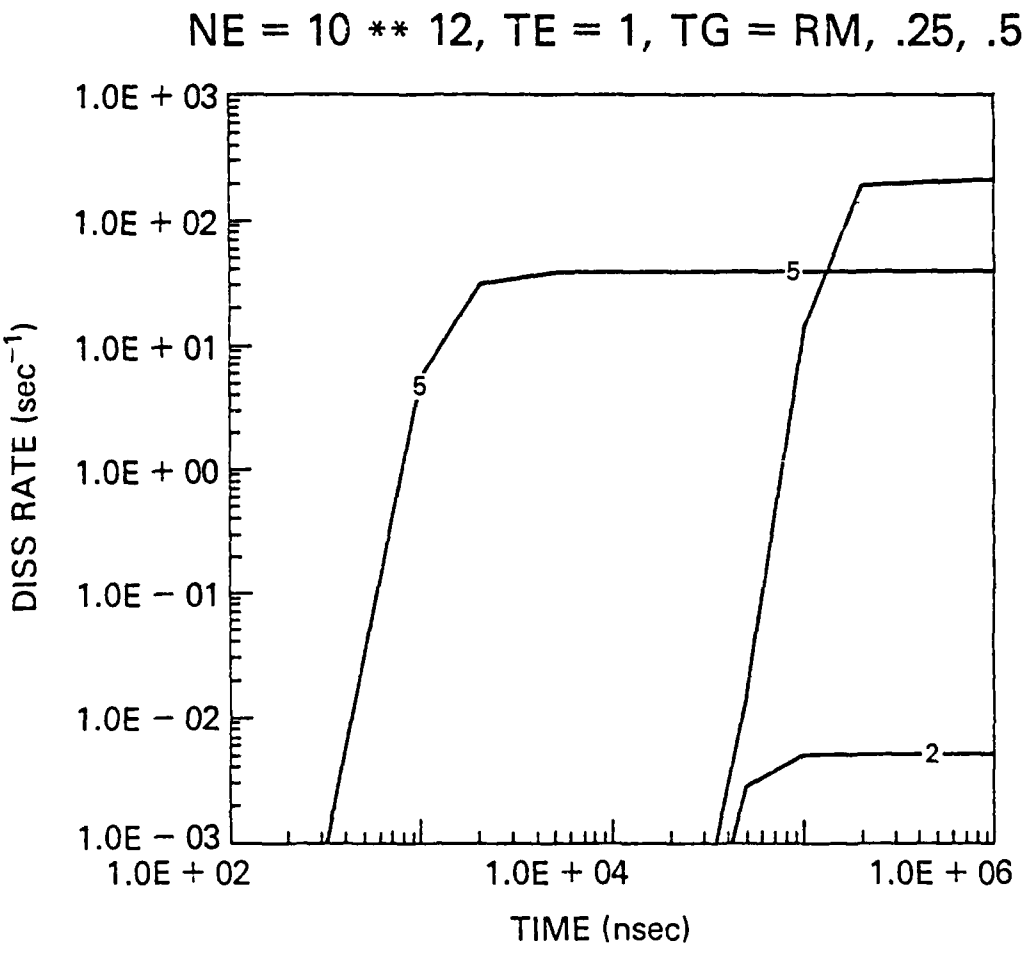

Fig. 19 The Dissociation Rate for $N_e = 10^{12}$, T_e = 1.0 eV and T_g = 0.025 eV, 0.25 eV and 0.5 eV

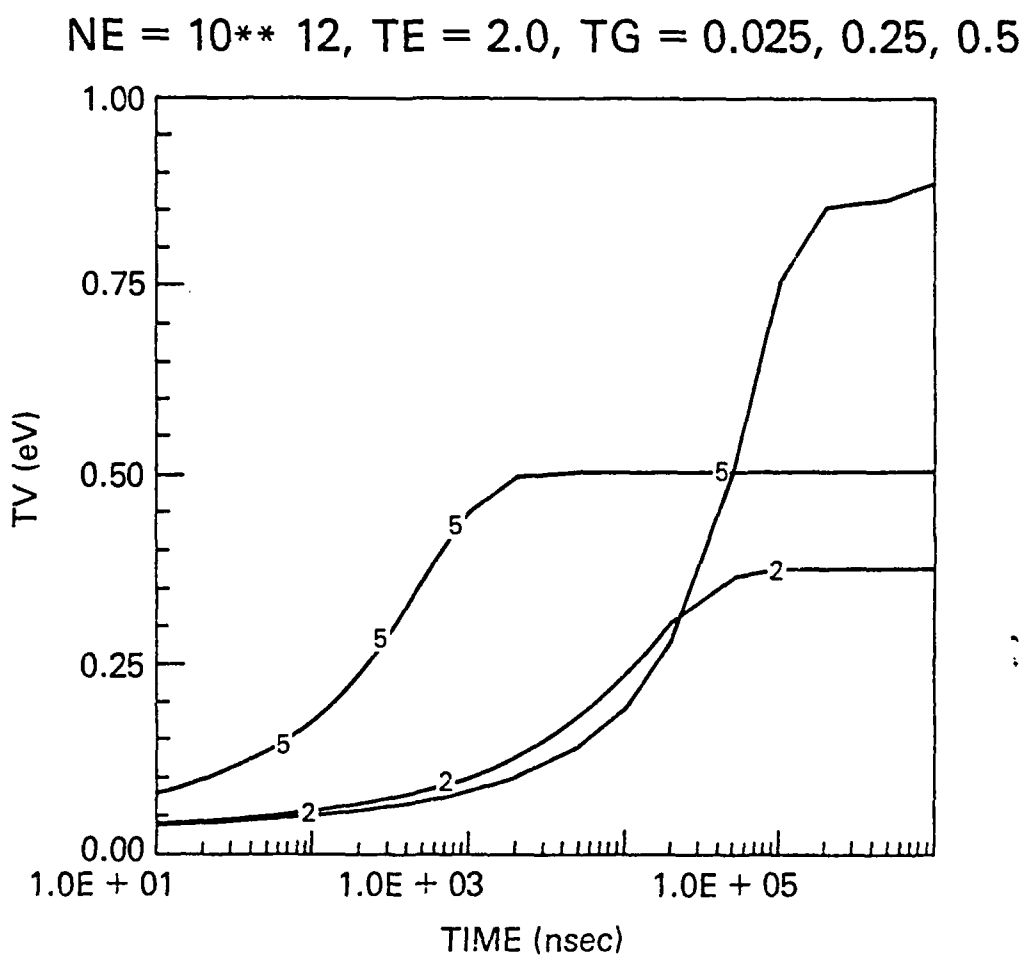

Fig. 20 The Vibrational Temperature for $N_e = 10^{12} cm^{-3}$, T_e = 1.0 eV and T_g = 0.025 eV, 0.25 eV and 0.5 eV

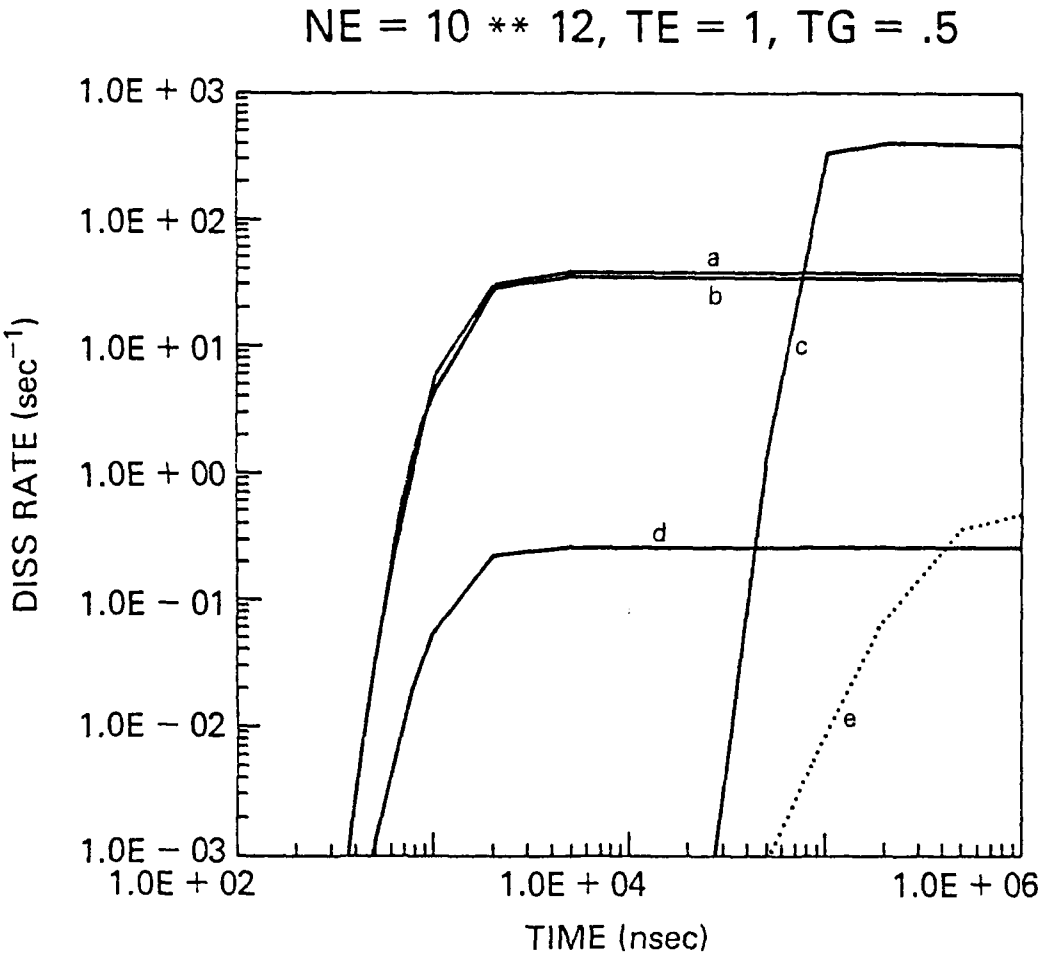

Fig. 21 The Dissociation Rate for $N_e = 10^{12}cm^{-3}$, T_e = 1.0 eV and T_g = 0.5 eV (a) all processes, (b) V-V and V-T only (c) e-V and V-V only (d) e-V and T-V only (e) e-V only

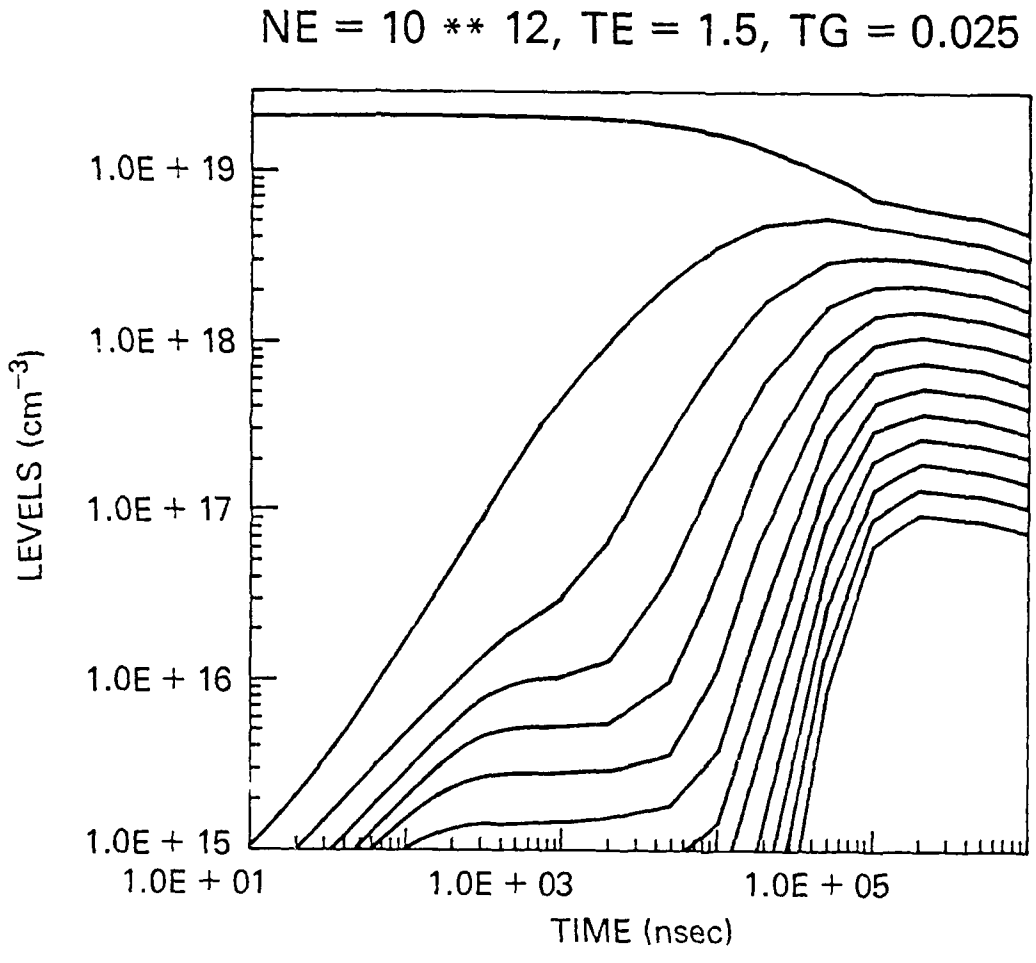

Fig. 22 Vibrational State Densities for $N_e = 10^{12} cm^{-3}$, T_e = 1.0 eV and T_g = 0.025 where only e-V processes are considered

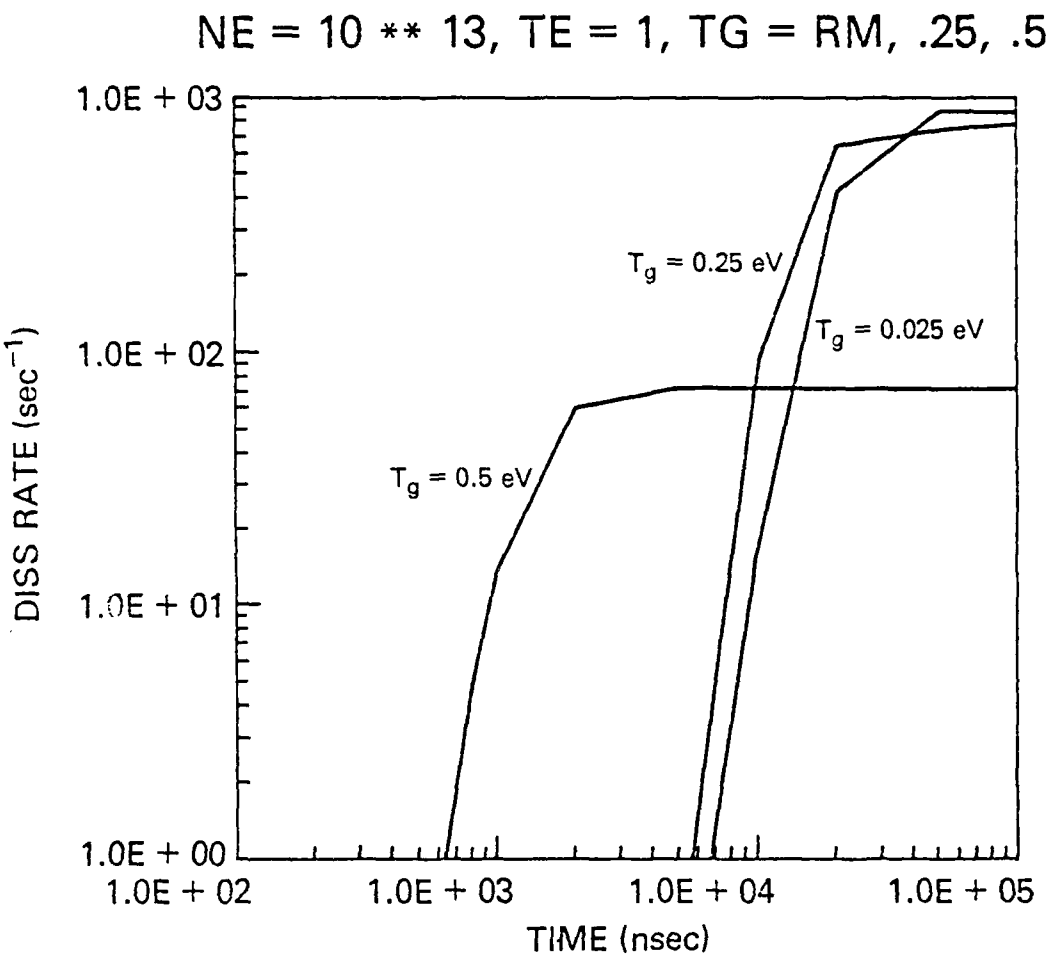

Fig. 23 The Dissociation Rate for $N_e = 10^{13} cm^{-3}$, T_e = 1.0 eV and T_g = 0.025 eV, 0.25 eV and 0.5 eV

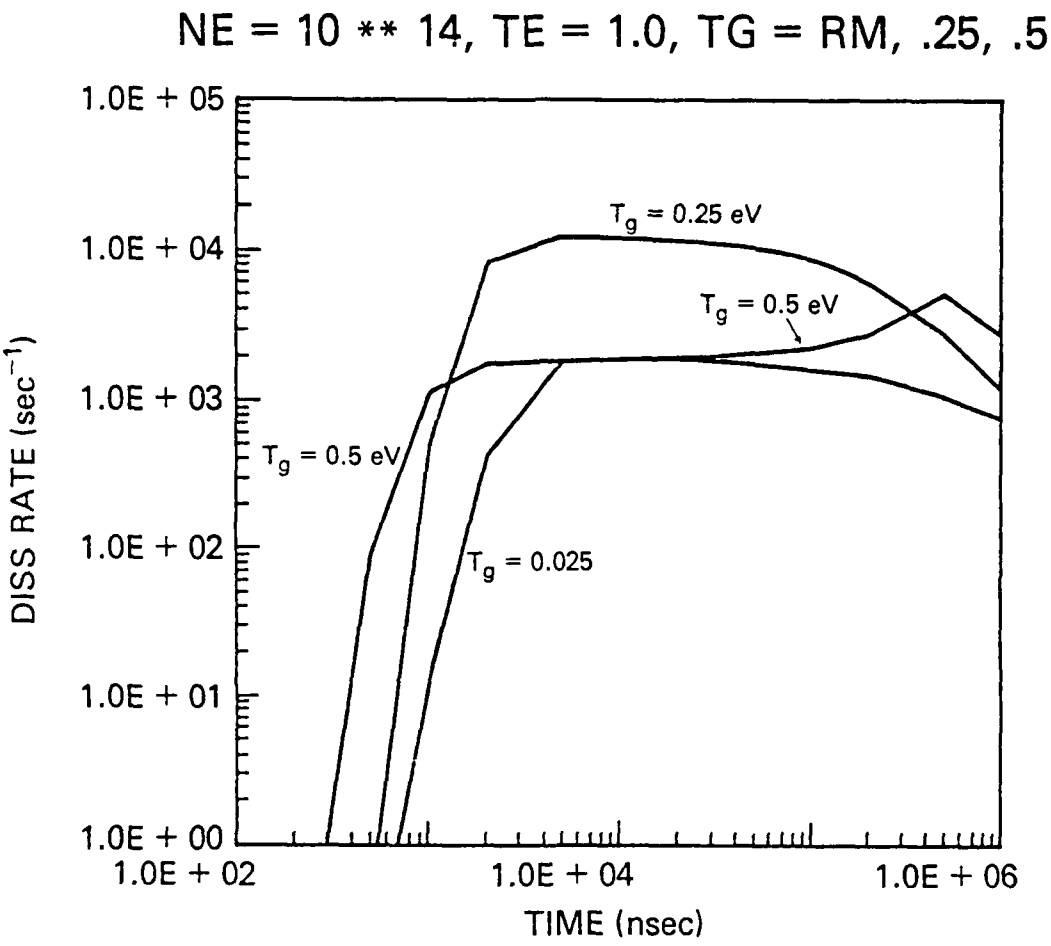

Fig. 24 The Dissociation Rate for $N_e = 10^{14} cm^{-3}$, T_e = 1.0 eV and T_g = 0.025 eV, 0.25 eV and 0.5 eV

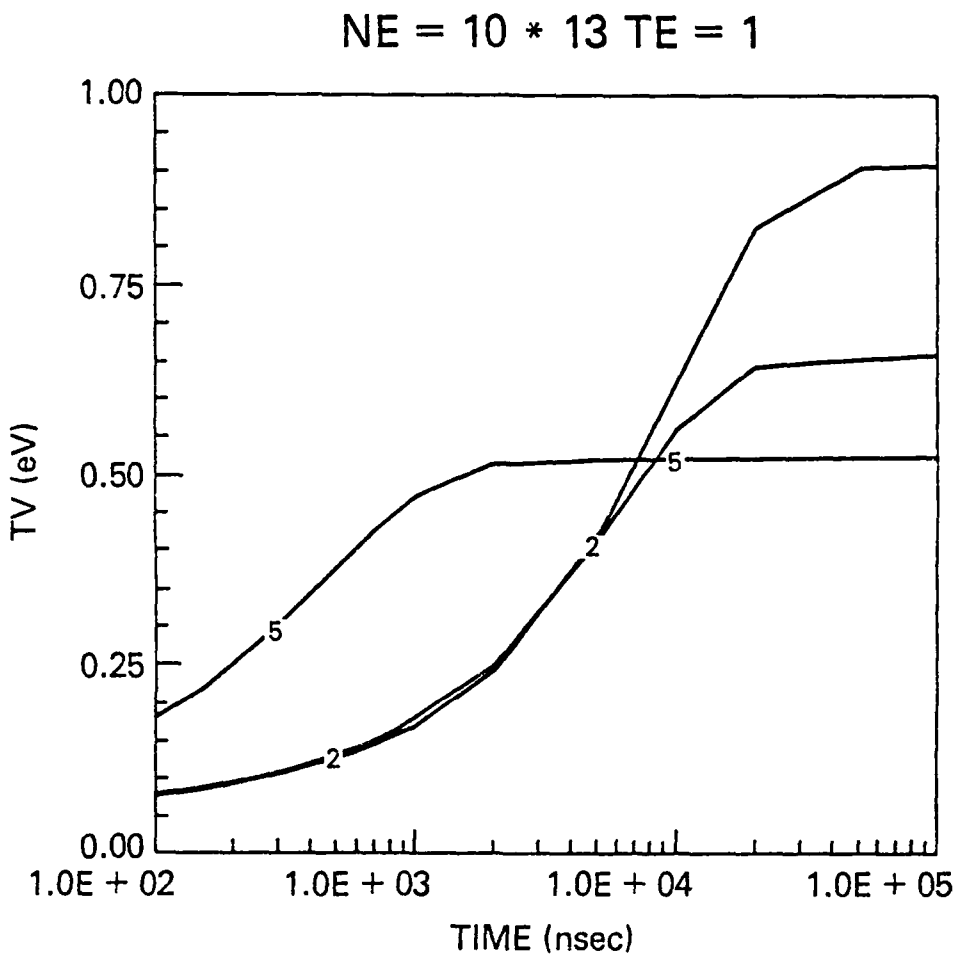

Fig. 25 The Vibrational Temperature for $N_e = 10^{13} cm^{-3}$, T_e = 1.0 eV and T_g = 0.025 eV, 0.25 eV and 0.5 eV

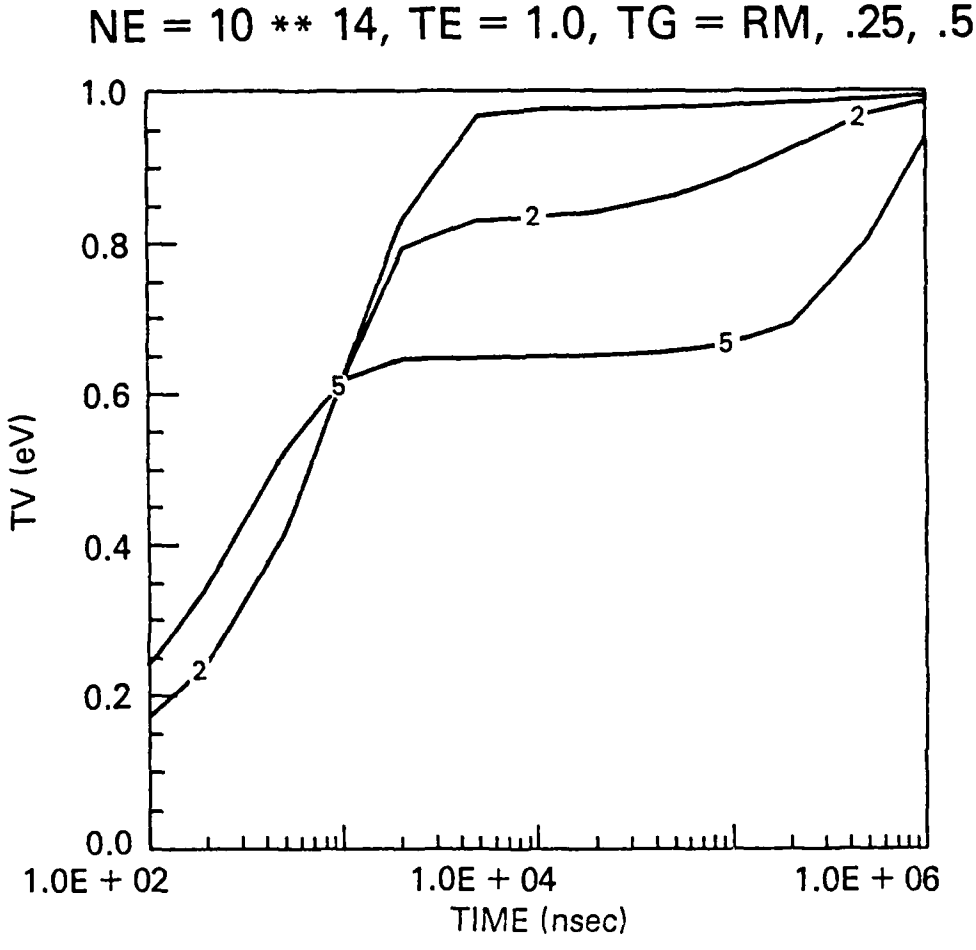

Fig. 26 The Vibrational Temperature for $N_e = 10^{14}cm^{-3}$, T_e = 1.0 eV and T_g = 0.025 eV, 0.25 eV and 0.5 eV

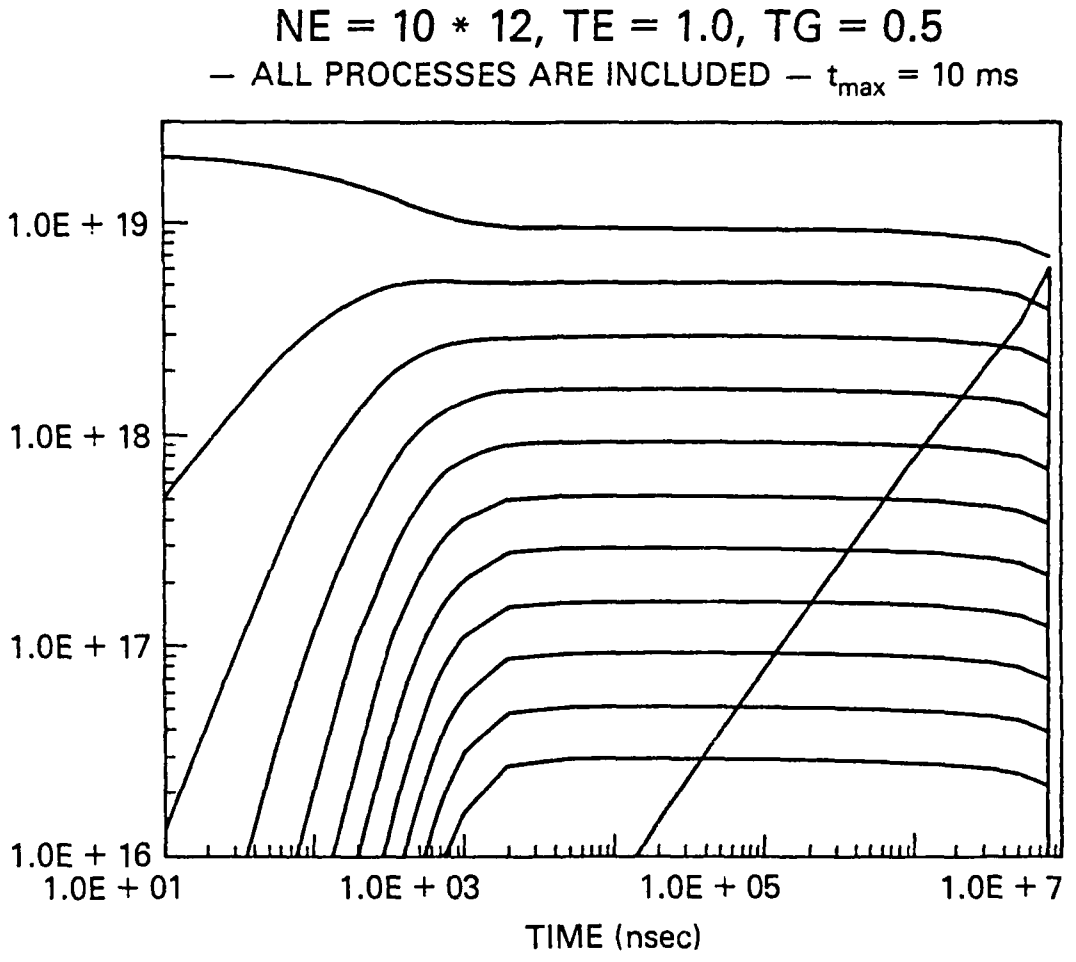

Fig. 27 Vibrational State Density for $N_e = 10^{12} cm^{-3}$, T_e = 1.0 eV and T_g = 0.5 eV. The steady state and the decay are indicated.

REFERENCES

1. R. C. Millikan and D. R. White J. Chem. Phys. 39, 3209 (1963) and references therein.

2. E. R. Fisher and R. H. Kummler, J. Chem. Phys. 49, 1075 (1968) ibid 49, 1085 (1968) and references therein.

3. J. H. Kiefer and R. W. Lutz, J. Chem. Phys. 44, 668 (1966) and references therein.

4. M. Capitelli and M. Dilonardo, Chem. Phys. 20, 417 (1977.

5. A. W. Ali and S. Slinker, proceedings, XVI Int. Conf. Phen. Ion. Gases Vol. 4, 596, Botticher, Wenk and Schulz-Gulde Eds., Dusseldorf (1983).

6. F. R. Gilmore, J. Quant. Spect. Rad. Transfer 5, 369 (1965).

7. G. J. Schulz, Phy. Rev. 135, A988 (1964) and references therein.

8. D. Spence, J. L. Mauer and G. J. Schulz, J. Chem. Phys. 57, 5516 (1972).

9. A. W. Ali and A. D. Anderson "Low Energy Electron Impact Rate Coefficeints for Some Atmospheric Species" NRL Report 7432 (1972), S. Slinker and A. W. Ali "Electron Excitation and Ionization Rate Coefficients for N_2, O_2, NO and O" NRL Memo. Report 4756 (1982). AD742-244 and AD A110-988

10. R. L. Taylor, Can. J. Chem. 52, 1436 (1974).

11. D. Rppp and P. Englander-Golden, J. Chem. Phys. 40, 573; ibid, 3120 (1964).

12. E. W. McDaniel "Collision Phenomena in Ionized Gases" Wiley (1964) New York.

13. H. F. Winters, J. Chem. Phys 44, 1472 (1966).

14. E. C. Zipf and R. W. McLaughlin, Planet Space Science 26, 449 (1978).

15. E. N. Lassettre in Methods of Experimental Physics, Ed. D. William Vol. 3 Part B p. 866, references therein, Academic Press, New York (1974).

16. P. K. Caroll and K. Yoshino, J. Phys. B5, 1614 (1972) and references therein.

17. R. D. Hudson and V. L. Carter, Can J. Chem. 47, 1840 (1969).

DISTRIBUTION LIST

Chief of Naval Operations
Washington, D.C. 20350
ATTN: Dr. C. F. Sharn (OP0987B)

U. S. Army Ballistics Research Laboratory
Aberdeen Proving Ground, Maryland 21005
ATTN: Dr. Donald Eccleshall (DRXBR-BM)
Dr. Anand Prakash

Office of Under Secretary of Defense
Research and Engineering
Room 3E1034
The Pentagon
Washington, D.C. 20301
ATTN: Mr. John M. Bachkosky

Office of Naval Research
800 North Quincy Street
Arlington, VA 22217
ATTN: Dr. C. W. Roberson

Chief of Naval Material
Office of Naval Technology
MAT-0712, Room 503
800 North Quincy Street
Arlington, VA 22217
ATTN: Er. Eli Zimet

Commander
Naval Sea Systems Command
PMS-405
Washington, D.C. 20362
ATTN: Capt. Robert L. Topping
Cmdr. W. Bassett

Air Force Office of Scientific Research
Physical and Geophysical Sciences
Bolling Air Force Base
Washington, D.C. 20332
ATTN: Capt. Henry L. Pugh, Jr.

Department of Energy
Washington, D.C. 20545
ATTN: Dr. Terry F. Godlove (C-404)
Dr. James E. Leiss (G-256)
Mr. Gerald J. Peters (G-256)

Joint Institute for Laboratory Astrophysics
National Bureau of Standards and
University of Colorado
Boulder, CO 80309
ATTN: Dr. Arthur V. Phelps

Lawrence Berkeley Laboratory
University of California
Berkeley, CA 94720
ATTN: Dr. Edward P. Lee

Ballistic Missile Defense Advanced Technology Center
P. O. Box 1500
Huntsville, AL 35807
ATTN: Dr. M. Hawie (BMDSATC-1)

Intelcom Rad Tech.
P. O. Box 81087
San Diego, CA 92138
ATTN: Dr. W. Selph

Lawrence Livermore National Laboratory
University of California
Livermore, CA 94550
ATTN: Dr. Richard J. Briggs
Dr. Thomas Fessenden
Dr. Frank Chambers
Dr. James W.-K. Mark, L-477
Dr. William Fawley
Dr. Jon Masamitsu
Dr. William Barletta
Dr. William Sharp
Dr. D. S. Prono
Dr. J. K. Boyd
Dr. K. W. Struve
Dr. John Clark
Dr. G. J. Caporaso
Dr. William E. Martin
Dr. D. Prosnitz

Mission Research Corporation
735 State Street
Santa Barbara, CA 93102
ATTN: Dr. C. Longmire
Dr. N. Carron

National Bureau of Standards
Gaithersburg, MD 20760
ATTN: Dr. Mark Wilson

Science Applications, Inc.
1200 Prospect Street
La Jolla, CA 92037
ATTN: Dr. M. P. Fricke
Dr. W. A. Woolson

Science Applications, Inc.
5 Palo Alto Square, Suite 200
Palo Alto, CA 94304
ATTN: Dr. R. R. Johnston
Dr. Leon Feinstein
Dr. Douglas Keeley

Science Applications, Inc.
1651 Old Meadow Road
McLean, VA 22101
ATTN: Mr. W. Chadsey

Naval Surface Weapons Center
White Oak Laboratory
Silver Spring, MD 20910
ATTN: Mr. R. J. Biegalski
Dr. R. Cawley
Dr. J. W. Forbes
Dr. D. L. Love
Dr. C. M. Huddleston
Dr. G. E. Hudson
Mr. W. M. Hinckley
Mr. N. E. Scofield
Dr. E. C. Whitman
Dr. M. H. Cha
Dr. H. S. Uhm
Dr. R. Fiorito

C. S. Draper Laboratories
Cambridge, MA 02139
ATTN: Dr. E. Olsson
Dr. L. Matson

Physical Dynamics, Inc.
P. O. Box 1883
La Jolla, CA 92038
ATTN: Dr. K. Brueckner

Office of Naval Research
Department of the Navy
Arlington, VA 22217
ATTN: Dr. W. J. Condell (Code 421)

Avco Everett Research Laboratory
2385 Revere Beach Pkwy
Everett, MA 02149
ATTN: Dr. R. Patrick
Dr. Dennis Reilly
Dr. D. H. Douglas-Hamilton

Defense Technical Information Center
Cameron Station
5010 Duke Street
Alexandria, VA 22314 (2 copies)

Mission Research Corporation
1720 Randolph Road, S.E.
Albuquerque, NM 87106
ATTN: Dr. Brendan Godfrey
Dr. Richard Adler
Dr. Thomas Hughes
Dr. Lawrence Wright

Princeton University
Plasma Physics Laboratory
Princeton, NJ 08540
ATTN: Dr. Francis Perkins, Jr.

McDonnell Douglas Research Laboratories
Dept. 223, Bldg. 33, Level 45
Box 516
St. Louis, MO 63166
ATTN: Dr. Michael Greenspan
Dr. Carl Leader

Cornell University
Ithaca, NY 14853
ATTN: Prof. David Hammer

Sandia National Laboratory
Albuquerque, NM 87115
ATTN: Dr. Bruce Miller
Dr. Barbara Epstein
Dr. John Freeman
Dr. John Brandenburg
Dr. Gordon T. Leifeste
Dr. Carl A. Ekdahl, Jr.
Dr. Gerald N. Hays
Dr. James Chang
Dr. Michael G. Mazerakis

University of California
Physics Department
Irvine, CA 92664
ATTN: Dr. Gregory Benford

Air Force Weapons Laboratory
Kirtland Air Force Base
Albuquerque, NM 87117
ATTN: D. Straw (AFWL/NTYP)
R. Lemke (AFWL/NTYP)
C. Clark (AFWL/NTYP)
W. Baker (AFWL/NTYP)
Lt. Col. J. Head

R&D Associates
P. O. Box 9695
Marina del Rey, CA 90291
ATTN: Dr. R. E. LeLevier

Pulse Sciences, Inc.
14796 Wicks Blvd.
San Leandro, CA 94577
ATTN: Dr. Sidney Putnam

Los Alamos National Scientific Laboratory
P. O. Box 1663
Los Alamos, NM 87545
ATTN: Dr. L. Thode
Dr. A. B. Newberger, X-3, MS-608
Dr. M. A. Mostrom, MS-608
Dr. T. P. Starke, MS-942
Dr. H. Dogliani, MS-5000

Western Research Corp.
8616 Commerce Avenue
San Diego, CA 92121
ATTN: Dr. Frank Felber

Institute for Fusion Studies
University of Texas at Austin
RLM 11.218
Austin, TX 87712
ATTN: Prof. Marshall N. Rosenbluth

University of Michigan
Dept. of Nuclear Engineering
An Arbor, MI 48109
ATTN: Prof. Terry Kammash
Prof. R. Gilgenbach

TRW Electronics and Defense Sector
One Space Park - R1/1078
Redondo Beach, CA 90278
ATTN: Dr. John R. Bayless

Directed Technologies, Inc.
226 Potomac School Road
McLean, VA 22101
ATTN: Dr. Ira F. Kuhn
Dr. Nancy Chesser

Titan Systems, Inc.
8950 Villa La Jolla Drive-Suite 2232
La Jolla, CA 92037
ATTN: Dr. H. L. Buchanon
Dr. R. M. Dowe

Naval Research Laboratory
Washington, D. C. 20375
ATTN: M. Lampe - Code 4792
M. Friedman - Code 4700.1
J. R. Greig - Code 4763
I. M. Vitkovitsky - Code 4701
J. B. Aviles - Code 4665
M. Haftel - Code 4665
T. Coffey - Code 1001
S. Ossakow - Code 4700 (26 copies)
P. Sprangle - Code 4790
Library - Code 2628 (20 copies)
A. W. Ali - Code 4700.1 (30 copies)
D. Book - Code 4040
J. Boris - Code 4040
I. Haber - Code 4790
B. Hui - Code 4790
S. Kainer - Code 4790
G. Joyce - Code 4790
D. Murphy - Code 4763
D. Colombant - Code 4790
M. Picone - Code 4040
M. Raleigh - Code 4760
R. Pechacek - Code 4763
Y. Lau - Code 4790

Defense Advanced Research Projects Agency
1400 Wilson Blvd.
Arlington, VA 22209
ATTN: Dr. J. Mangano
Lt. Col. R. L. Gullickson

JAYCOR
5705A General Washington Drive
Alexandria, VA 22312
ATTN: Dr. D. Tidman
Dr. R. Hubbard
Dr. S. Slinker

Physics International, Inc.
2700 Merced Street
San Leandro, CA 94577
ATTN: Dr. E. Goldman

Standford Linear Accelerator Center
P. O. Box 4349
Stanford, CA 94305
ATTN: Dr. Simon S. Yu

Lockheed Palo Alto Laboratory
3251 Hanover Street
Bldg. 203, Dept. 52-11
Palo Alto, CA 94304
ATTN: Dr. John Siambis

University of Maryland
Physics Department
College Park, MD 20742
ATTN: Dr. Y. C. Lee
Dr. C. Grebogi

Maxwell Laboratories, Inc.
8835 Balboa Avenue
San Diego, CA 92123
ATTN: Dr. Nino Pereira

Science Applications, Inc.
1710 Goodridge Drive
McLean, VA 22102
ATTN: Dr. A. Drobot
Dr. K. Papadopoulos